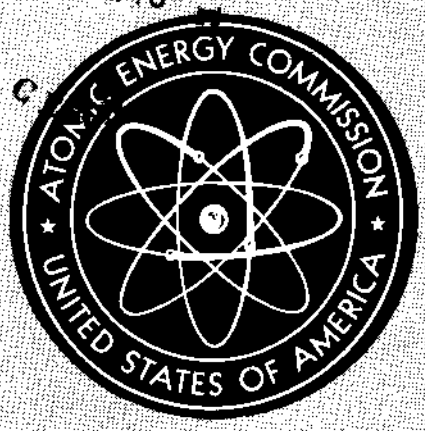

HASL-258

IN SITU Ge(Li) AND NaI(Tl) GAMMA-RAY SPECTROMETRY

September 1972

Health and Safety Laboratory (AEC)
New York, New York

UNITED STATES ATOMIC ENERGY COMMISSION • TECHNICAL INFORMATION CENTER

NOTICE

Printed in the United States of America
USAEC Technical Information Center, Oak Ridge, Tennessee

HEALTH AND SAFETY (TID-4500) HASL-258

IN SITU Ge(Li) AND NaI(Tl) GAMMA-RAY SPECTROMETRY

Harold L. Beck
Joseph DeCampo
Carl Gogolak

September 1972

Health and Safety Laboratory
U. S. Atomic Energy Commission
New York, New York 10014

ABSTRACT

The use of large NaI(Tl) crystals and large Ge(Li) diodes to make *in situ* measurements of γ-rays from sources in the soil and air is described. Methods for inferring source concentrations and contributions to the total exposure rate from individual emitters are discussed and tables of photon flux to source activity and flux to exposure rate conversion factors are presented. Descriptions are given of the calibration of 4 in. by 4 in. NaI(Tl) detectors, and 25 cm^3 and 60 cm^3 Ge(Li) diodes. A number of applications of field spectrometry are discussed.

TABLE OF CONTENTS

TABLE OF CONTENTS (Cont'd)

TABLES

TABLE OF CONTENTS (Cont'd)

TABLE OF CONTENTS (Cont'd)

TABLE OF CONTENTS (Cont'd)

Page

ILLUSTRATIONS

I. INTRODUCTION

The Health and Safety Laboratory (HASL) pioneered the development of *in situ* gamma-ray spectrometric techniques, first utilizing large NaI(Tl) crystals[1,2] and later Ge(Li) diodes[3]. These spectra are used to provide information on the identity of radionuclides in the soil and air, their concentrations in the soil and their individual exposure rate contributions[4,5].

In situ measurements of soil activity are more sensitive and provide more representative data than data obtained by sample collection and subsequent laboratory analysis. An unshielded detector placed about one meter above the ground detects gamma rays from an area within about a 10 meter radius, representing a large volume of soil compared to the typical soil sample, and comparable counting statistics can be obtained in only a small fraction of the time required for the laboratory analysis. For example, a field spectral analysis for the natural emitters, ^{40}K, ^{238}U and ^{232}Th, can be carried out in approximately 15 minutes with a 4 in. by 4 in. NaI(Tl) detector. A comparable analysis in the laboratory, excluding transportation and sample preparation time, would require several hours. Furthermore, a single soil sample from a site may not be representative of the mean soil activity, so a number of samples or composite samples are required. A single field analysis averages out small local inhomogeneties in the sample.

The most important disadvantage of *in situ* spectrometry is that the accuracy of the analysis depends on a separate knowledge of the radioactivity distribution with soil depth, and to a lesser extent a knowledge of the soil density, moisture content and chemical composition. We will show, however, that exposure rate estimates are much less sensitive to variations in radionuclide distribution and soil characteristics than are concentration estimates and that very accurate estimates of individual nuclide contributions to the total external exposure rate can be made from the field spectra.

Our NaI(Tl) analysis techniques have been discussed extensively in prior publications[1-5], and similar work has since been reported by other investigators[6-9]. The specific application of our analysis to large lithium drifted germanium diodes [Ge(Li)] has only qualitatively been discussed[3]. In addition, since our last detailed report on spectrometric methods[5], improved calculations of gamma-ray flux and exposure rate in air as a function of soil concentration have been made, and new and more precise information on the gamma-ray emissions of ^{226}Ra and ^{232}Th daughters has become available. These new data have allowed us to improve the flux to dose conversions used in our spectral analysis.

II. EXPERIMENTAL EQUIPMENT; FIELD PROCEDURES

Figure 1 is a block diagram of our field equipment arrangement. Each detector is placed on a tripod, facing downward toward the soil halfspace, at a distance of 1 meter above the ground (Figure 2). The site is usually chosen to be a flat relatively undisturbed area whose soil is typical of the surrounding environs. We have found that this measurement technique smooths out much of the effect of ground roughness. Extreme roughness will result in anomalies since the soil surface area close to the detector is increased, while the surface contribution from large distances is reduced.

The NaI detectors are usually covered (in addition to the manufacturers standard thin aluminum or stainless steel window) by a 1/4 in. bakelite shield to reduce the beta-ray contribution to the Compton continuum as well as to moderate thermal stresses.

The NaI detectors (usually 4 in. by 4 in. cylindrical crystals attached to 3 in. matched photomultiplier tubes) are coupled through an emitter-follower preamplifier and a 100 ft. coaxial cable to a multichannel analyzer in our field vehicle. The output of the Ge(Li) diode goes to an uncooled preamplifier directly attached to the cryostat, then through a specially designed low noise 100 ft. cable carrying the

preamplifier power and transmitting the signal to a high resolution amplifier and 4000 channel analyzer in the vehicle. The 5 liter dewar attached to the diode-cryostat requires filling every four days and for long trips an extra 30 liter dewar of liquid nitrogen is carried along. The electronic equipment is shockmounted in a rack mounted in a station wagon (Figure 3). Power for operating all the equipment for up to eight hours is supplied by three 95 ampere-hour storage batteries coupled to a solid-state 12 V DC-AC converter. The primary output device is a magnetic tape recorder, however, a parallel printer is also available. The particular analyzer we use was chosen for its low power requirements (~200 watts), its compact size, weight and acceptable temperature stability characteristics.

The Ge(Li) and NaI(Tl) detectors, when not in use, are transported in rugged styrofoam cushioned boxes designed to minimize both mechanical and thermal shock. Portable lead shielding also allows us to use the detectors for counting samples in a fixed geometry in the field.

NaI(Tl) spectra are usually accumulated in from 10 - 20 minutes while Ge(Li) spectra usually require from 30 to 90 minutes counting time depending on the soil activity and active volume of the diode. Although the resolution obtainable in the field is not usually as good as that in the laboratory, we rarely encounter significant deterioration in resolution from gain or zero drift even during very warm or cold days because of the relatively short counting intervals. We use no special gain stabilization equipment. The detector characteristics are discussed more fully in Section V of this report.

Our standard practice at each measurement site is to first monitor the entire area with hand-held, NaI scintillation meters to assure that the radioactivity level is relatively uniform. A high pressure ionization chamber[10] is used to measure the total exposure rate at the site.

III. THE ANALYSIS OF IN SITU SPECTRA

The total absorption peaks in a spectrum are a measure of the gamma-ray flux of a particular energy incident on the detector. By calibrating the detector in the laboratory with standard point sources we have determined the detector response in terms of total absorption peak counts for a given flux as a function of gamma-ray energy and angle of incidence. The area of a total absorption peak in a field spectrum is thus a measure of the actual flux incident on the detector in the field situation. We have also calculated the expected flux at the detector per unit activity of each nuclide in the soil for various source depth distributions and soil properties and obtained theoretical flux to concentration ratios. We extended the method to exposure rate estimates by calculating the total exposure rate expected at various heights above the ground per unit activity of a particular nuclide in the soil, obtaining theoretical flux to exposure rate ratios. Multiplying the absorption peak area response of the detector per unit incident flux by the calculated flux to exposure rate and flux to activity ratios we obtain calibration factors in terms of total absorption peak counts per μR/hr or per pCi/gm for each nuclide of interest.

We can describe the analysis symbolically in the following manner. Let

(N_0/φ) = an estimate of the counts per minute obtained under a particular spectrum total absorption peak due to a unit flux of gamma rays of energy E incident on the detector parallel to the axis of symmetry of the detector.

(N_f/N_0) = the angular correction factor applied to (N_0/φ) to account for the fact that gamma rays in the field situation are not incident parallel to the detector axis of symmetry. If the detector has a uniform response over the solid angle from which gamma rays enter the detector in the field, then $N_f/N_0 = 1.0$. If not, the measured angular response of the detector

must be integrated over the actual distribution. This latter quantity is a function of energy, source distribution, soil density, and soil composition.

(φ) = total flux at the detector per unit soil concentration [(pCi/g) or (mCi/km^2)] of a particular nuclide as a function of energy, source distribution, and soil properties.

(I) = exposure rate in $\mu R/hr$ at one meter above the ground from all gamma rays originating from a particular nuclide and the secondaries produced in the soil and air.

(φ/I) = the ratio of the flux at the detector due to gamma rays of energy E emitted as a result of the decay of a particular nuclide and any daughters to the corresponding exposure rate for that nuclide and its daughters in equilibrium, if specified.

Then, the absorption peak counting rate is related to the exposure rate in air above the ground or to radionuclide concentration in the ground by

$$(N_f/I) = (N_f/N_o)(N_o/\varphi)(\varphi/I) = \text{peak area counts per } \mu R/hr,$$

$$(N_f/A) = (N_f/N_o)(N_o/\varphi)(\varphi/A) = \text{peak area counts per minute per pCi/g or } mCi/km^2.$$

This analysis is equally applicable to NaI(Tl) and Ge(Li) detectors, though the estimation of absorption peak areas for the two types of detectors are quite different. The very great resolution of Ge(Li) detectors allows one to measure absorption peak areas due to a given gamma-ray transition with very little interference from neighboring peaks. Often, the areas of several peaks resulting from the same nuclide may be measured. The efficiency of Ge(Li) diodes is still much lower than NaI(Tl) and thus longer counting times are required to obtain comparable statistical precision. The poorer resolution of the NaI(Tl) data often makes difficult the estimation of absorption peak area due to interference from nearby peaks.

Though our calibration data on N_o/φ and N_f/N_o are strictly valid only for our particular detectors, except for nominal differences in volume, our NaI(Tl) data should be applicable to other 4 in. by 4 in. detectors and our Ge(Li) data should be instructive in illustrating the differences in NaI and Ge(Li) sensitivity.

The calculations of φ, φ/A, φ/I, and I given in the next section, however, are generally useful for any detector calibration.

IV. CALCULATIONS OF FLUX AND EXPOSURE RATE

Gamma-Ray Flux from Monoenergetic Sources in the Soil

The total flux of gamma rays of energy E at height h cm above a flat air-ground interface due to an emitter distributed in the soil exponentially with depth is given by

$$\varphi(r,\theta) = 2\pi \int_o^{\pi/2} \int_{h/\omega}^{\infty} \frac{S_o}{4\pi r^2} \exp[-(\alpha/\rho)\rho z]r^2 \sin\theta \exp[-\mu_s(r-h/\omega)] \cdot \exp[-\mu_a(h/\omega)]\, dr\, d\theta, \qquad (1)$$

where

r = the distance from each element of differential volume to the detector position,

$\omega = \cos\theta$,

Z = the depth beneath the surface in cm,

S_o = the surface activity, photons/sec-cm^2,

α = the reciprocal of the relaxation length of the assumed exponentially-distributed source activity with depth, cm^{-1},

ρ = soil bulk density, g/cm^3, and

μ_a, μ_s = the air and soil total gamma-ray attenuation coefficients, cm^{-1}.

The dependence of φ on the photon angle of incidence with respect to the perpendicular to the earth-air interface, θ, is obtained by integration over r, hence

$$\varphi(\omega) = \frac{S_o/\rho}{2}\left[\frac{1}{(\alpha/\rho)\omega + (\mu_s/\rho)}\right] \exp(-t/\omega) \qquad (2)$$

where

S_o/ρ is the surface activity per unit mass of soil and the activity at depth ρz g/cm^2 is given by $S/\rho = S_o/\rho \exp(-\alpha/\rho \cdot \rho z)$, and

μ_s/ρ is the mass attenuation coefficient for soil and t is the height of the detector above the interface in units of mean free paths of air, i.e. $t = (\mu_a/\rho_a)(h\rho_a)$.

Since

$$S_A = \int_o^\infty \rho \frac{S_o}{\rho} \exp(-\alpha/\rho \ \rho z)\ dz = S_o/\alpha$$

is the total activity in an infinitely deep column of soil of unit cross-sectional area, then equation (2) can be rewritten

$$\varphi(\omega) = \frac{\alpha S_A}{2\rho} \exp(-t/\omega)\left[\frac{1}{(\alpha/\rho)\omega + (\mu_s/\rho)}\right] \qquad (3)$$

Equations (1-3) give the flux in air at any height t for a source distributed exponentially in the soil as long as we

are dealing with infinite half-space geometry, i.e. as long as variations occur only in the z direction. Any depth distribution can be represented by a superposition of plane sources buried at various depths and equations (1-3) merely represent particular superpositions. For most real situations the actual distribution of activity can be represented by equations (2) and (3). Natural emitters are usually distributed reasonably uniformly in the soil; for this case $\alpha/\rho = 0$ and equation (2) becomes

$$\varphi(\omega) = [(S_o/\rho)/2(\mu_s/\rho)] \exp(-t/\omega) \qquad (4)$$

and the total flux,

$$\varphi = \int_o^1 \varphi(\omega)\, d\omega. \qquad (5)$$

Equation (5) generally cannot be evaluated directly but can be solved numerically with the aid of a large computer.

For a plane source on the soil surface, representative of fresh weapons fallout, $\alpha/\rho \to \infty$ and from equation (3) we obtain

$$\varphi(\omega) = \frac{S_A}{2\omega} \exp(-t/\omega) \qquad (6)$$

and the total flux,

$$\varphi = \int_o^1 \varphi(\omega)\, d\omega = \frac{S_A E_1(t)}{2}, \qquad (7)$$

where $E_1(t)$ is the exponential integral, sometimes also written $-E_i(-t)$. The values of $E_1(t)$ have been tabulated in many mathematical handbooks.

Fallout deposited on the ground tends to approach a distribution which can be reasonably approximated by an

exponential distribution after some time[11]. The value of α/ρ best describing the distribution will depend on the type of soil, soil density and moisture content. Values of α/ρ ranging from 0.05 to 0.5 have been found to describe realistic fallout distributions adequately, the more aged fallout, of course, being represented by the smaller values[11].

Calculated Fluxes

Using equations (2) and (3) we have calculated the unscattered photon flux at one meter above the interface for values of α/ρ ranging from 0 to ∞. These results are given in Table 1 for various monoenergetic source energies, for a source strength of S_A = 1.0 photons/cm^2-s except for the case of α/ρ = 0 (uniform) where the results are for S/ρ = 1.0 photons/s per gram of soil. We used the soil composition given in Table 2.

The choice of doing the $\alpha/\rho \neq 0$ calculations for a fixed total source activity and a varying source depth distribution rather than for a fixed value of surface activity ($S_o/\rho = \alpha S_A/\rho$) results in the $\alpha/\rho = 0$ data not being directly comparable to the $\alpha/\rho \neq 0$ data as tabulated. The effect of source depth distribution is more apparent from this type of normalization, however. The results could be re-normalized by letting S_o/ρ = 1.0 photon/g-s for all cases.

In Table 3 we give the fluxes at 1 meter for some typical fallout radionuclides obtained by interpolating the data in Table 1 and multiplying by the given photons/dis. In Table 4 we give similar results for the major ^{238}U and ^{232}Th transitions. The ^{238}U and ^{232}Th decay chains are listed in Table 5.

Dependence of Flux on Soil Density

Although soil densities may vary considerably from site to site, it can be seen from equations (3) and (4) that the soil density enters only in the terms α/ρ and μ_s/ρ. One can obtain the flux for any soil density from the flux vs. (α/ρ) in Table 1 since the quantity μ_s/ρ is independent of density

and depends only on isotopic composition. Although we typically assume a soil density of 1.6 g/cm^3, the values in Table 1 for any values of ρ and α are equally valid for other values of ρ as long as α/ρ = constant, i.e. the values given for α = 0.5 cm^{-1} and ρ = 1.6 correspond to the values for α = 1.0 cm^{-1} and ρ = 3.2. The values given for α/ρ = 0 depend only on the source activity per gram of soil material and not the actual soil density.

Angular Distribution of Flux

In Table 6 we give integral angular flux distributions obtained by integrating equation (1) from 0° to θ. From these data it is seen that most of the unscattered gamma rays incident on a detector at one meter above the ground arrive at angles of roughly from 50° - 80° from the vertical, i.e. are originating from an area bounded by radii of about 1 to 5 meters. Also for an energy of 662 keV and a relaxation length of 3 cm (α/ρ = 0.21) 85% of this flux comes from an area of about 10 meters in diameter. The area "seen" by the detector depends on the height of the detector, of course, as well as on the depth distribution (α/ρ) and to a much lesser extent on the gamma energy of the source.

Dependence of Flux on Soil Composition and Moisture Content

The unscattered flux is not completely independent of μ_s/ρ, the total mass attenuation coefficient of the soil. This quantity depends on the soil composition which itself depends on the soil moisture content. For a fairly wide range of soil contents, however, μ_s/ρ varies over a narrow range, as shown in Table 2. Since for the worst case, a uniformly distributed source as shown in equation 4, the flux varies only as $1/(\mu_s/\rho)$ and since μ_s/ρ changes by at most about 6 - 7% between aluminum and soil with 25% moisture content (Table 2), clearly a knowledge of the exact soil composition is not critical for the calculation of flux. A soil with a significant high Z material content could result in somewhat lower fluxes than are given in Tables 1, 3 and 4, however.

Dependence of Flux on Source Depth Distribution

It can be seen from Table 1 that the flux is strongly dependent on depth distribution, changing for example by almost an order of magnitude at 662 keV (see Table 1) as the source distribution changes from a plane source to a deeply distributed source. Increased soil moisture effectively results in a more deeply distributed source since increased soil moisture increases the density and thus reduces α/ρ.

Clearly, the relation of an *in situ* flux measurement to total soil concentration requires a fairly good knowledge of the effective depth distribution. Several possible ways come to mind for inferring the depth distribution from measurements of flux. One might infer the depth parameter, α/ρ, from measurements of flux at some energy at several heights above the soil. Unfortunately, the variation of flux with detector height is very insensitive to α/ρ over the first few meters above the interface[12]. For example, the ratio of 662 keV flux at 10 m to that at 1 m for $\alpha/\rho = 0.0625$ is 0.74, while for $\alpha/\rho = 0.1875$ it is 0.70[12].

An alternative might be to observe the photon flux at two different energies from the same source, e.g. 587 keV and 1596 keV from ^{140}La, or to assume the same depth distribution for say ^{141}Ce and ^{106}Ru (134 keV and 619 keV) which have similar half-lives. From Table 1 we see, however, that the ratio of the 150 keV flux to the 662 keV flux for $\alpha/\rho = 0.21$ is 0.68, while for $\alpha/\rho = 0.063$ it is 0.61, only about a 10% difference in α/ρ for very different photon energies. It is, in fact, very difficult to use measurements of total flux alone to determine α/ρ except perhaps in a very gross manner. This, of course, limits the ability of the field spectrometric method with respect to determining cumulative fallout soil activities unless one has some independent knowledge of the depth distribution. From Table 6, however, we note that the angular flux distributions are somewhat more sensitive to α/ρ and perhaps measurements of this quantity with collimated detectors could be used to infer approximate values of α/ρ.

Exposure Rates for Monoenergetic Sources in the Soil

The total exposure rates at 1 meter per unit concentration of source activity in the soil for monoenergetic sources as a function of source energy are given in Table 7. These data include the contributions from gamma rays scattered in both the soil and air and were determined utilizing a polynomial solution to the gamma-ray transport equation[12] for the soil composition given in Table 2 and a moisture content of 10% by weight.

Dependence of Exposure Rate on Soil Density

Like the flux the exposure rate is dependent on soil density and composition. The exposure rate due to a source of strength $S_o/\rho \exp(-\alpha/\rho\ \rho Z)$ buried at a depth between z and z + dz centimeters beneath the surface depends only on the number of mean free paths (MFP) to the interface, i.e.

$$I(h) \propto \int_o^\infty S_o\ F(\mu/\rho,\ \rho z,\ h)dz \qquad (8)$$

where I is the exposure rate at h meters above the interface and F is a quantity which relates the exposure at h to a plane source at depth z. F depends only on the number of gamma mean free paths $(\mu/\rho)\ (\rho z)$ between the height h and the depth z since the exposure rate from a buried plane source can be shown to be only a function of $\mu z = (\mu/\rho)(\rho z)$[12]. Equation (8) can be rewritten

$$I(h) \propto \int_o^\infty \frac{S_o/\rho}{\mu_s/\rho} F(MFP)d[(\rho z)(\mu/\rho)] = \int_o^\infty \frac{\alpha/\rho\ S_A}{\mu_s/\rho} F(MFP)d(MFP). \qquad (9)$$

As was the case for flux the exposure rate for a given S_A varies as α/ρ and one can obtain the value for any soil density by utilizing the Table 7 values with an appropriate value of α/ρ.

Dependence of Exposure Rate on Soil Composition and Moisture Content

The soil density at a given location may vary with time due to changes in soil moisture and α may remain constant or vary extremely slowly. Since μ_s/ρ increases only slightly with increasing water content (Table 2), the effect is to reduce the flux and exposure rate somewhat, since in effect each source element is further away from the detector in terms of mean free paths. For $\alpha/\rho = 0$, a uniformly distributed source, an increased moisture content reduces the source per gram of soil (or per MFP) and the exposure rate and flux are both reduced proportionately.

The above discussion assumed a uniform change in soil moisture content over the first several inches of soil, which may not be a realistic assumption for actual soils. In any case, both the flux and exposure rate should change about the same amount for most situations.

Since μ_s/ρ is not completely invariant small changes in the values of calculated exposure rates would result from the actual soil composition being different from that given in Table 2. However, our calculations indicate that these differences for most plausible soils are almost always less than 5% which is the same order as the error in the calculations[12]. Again, however, a soil rich in high Z material would not be represented as well by the exposure rate data in Table 6.

Exposure Rates for Natural and Fallout Emitters

The exposure rates at 1 meter for naturally-occurring radionuclides found in the soil are given in Table 8 while those for fallout emitters are given in Table 9. These data were calculated by folding together interpolated values from Table 7 with the best available data for the number of photons emitted per disintegration at each energy. The data for the fallout nuclides were taken from the Nuclear Data Tables[13] while those for the ^{238}U and ^{232}Th series are based primarily on recent measurements by Gunnink et al.[14],

Lingeman[15], Mowatt[16], and Maria et al.[17] as well as our own measurements with a Ge(Li) diode[12]. Our estimate of the best available gamma emission data for the major lines of the ^{238}U and ^{232}Th series are given in Table 4. These data differ considerably both from the data we used in the past[1,12] and that given by Hultquist in his early work[10] and the calculated exposure rate to concentration factors for ^{238}U and ^{232}Th, therefore, differ somewhat from those in our previous publications[1,2,4,5] (see Table 8). In addition, our earlier work[1] was based on a buildup factor calculation of the exposure rate which neglected differences between gamma-ray transport in air and soil. The approximate error resulting from the latter treatment can be seen in Table 10 for the case of a uniformly distributed source when we compare exposure rates calculated from transport theory with those calculated using the simple single medium buildup factor approach. As can be seen, the differences are only about 10% except for very low energies.

Although our new exposure rate per unit soil activity conversion factors for both ^{238}U and ^{232}Th are smaller than those used previously, implying that the exposure rates calculated at one meter from measured soil activity are somewhat less than previously thought, the total change in the ^{238}U series factor is only about 20% and in the ^{232}Th factor about 15%. Since our values for φ and N_0/φ have also been revised, our earlier estimates of exposure rates based on in situ spectral measurements are probably in error by less than these amounts.

Dependence of Exposure Rates on Radioactive Equilibrium of the ^{238}U and ^{232}Th Series - Radon Emanation

In using these conversion factors one should remember that they refer to concentrations in in situ soil and not in the dry sieved soil which is usually measured in the laboratory. Soil moisture content by weight of 10 - 20% seems to be fairly typical in the Eastern United States with wide variations from soil to soil.

The calculations also assumed that all daughters are in radioactive equilibrium with their parents. Actually, some fraction of the radon and thoron produced (see Table 5)

emanates from the soil matrix, diffuses through the soil air to the interface and then disperses throughout the atmosphere. The escape of ^{222}Rn is much more likely than that of ^{220}Rn because of its much longer half-life. The fraction of radon which escapes *in situ* soil, or emanation coefficient, varies considerably from soil to soil, typical values being about 20 - 30% although values as high as 50% are not uncommon[20,21]. Since most of the exposure rate from the ^{238}U series is from radon daughters (see Table 4), we can, to a good approximation, assume that the fraction of radon escaping into the soil air and then to the atmosphere will result in an equivalent reduction in gamma exposure rate at 1 meter. Under a steady-state condition, there will be some small contribution from this fraction whose source distribution can be represented by two exponential distributions, one in the atmosphere and one in the soil. For normal atmospheric diffusion and typical surface level radon air concentrations, we estimate this contribution to be only a few tenths of a μR/hr. During an inversion, however, the exposure rate would, of course, be somewhat increased since the radon would remain closer to the interface.

Errors would result when using a field measurement of the ^{214}Bi or ^{214}Po photon fluxes to estimate ^{238}U soil concentration or a laboratory measurement of equilibrium ^{238}U soil concentration to evaluate the one meter exposure rate. In these cases one would need to know both the emanation fraction and the approximate exposure rate contributions from radon in the soil air and atmosphere. The field spectrometric determination of exposure rate utilizes the ratio of flux to exposure rate and since both quantities contain a contribution from the emanated radon, the exposure rate estimate obtained by using a slightly incorrect value for φ/I would not be expected to be greatly in error. Indeed, as the radon builds up in the soil or near the ground due to increased soil moisture, frozen ground, or an atmospheric temperature inversion, the actual ratio of φ/I will approach the value used routinely (the equilibrium infinite half-space value) and the error in determining the exposure rate will be even smaller.

Disequilibrium in the ^{238}U series and ^{232}Th series can be investigated using field Ge(Li) spectra. For the ^{238}U

series one can obtain flux estimates from the 186 keV ^{226}Ra line as well as from lines of radon daughters and thus obtain rough estimates of the emanation fraction. Similarly, any disequilibrium in the ^{232}Th series can be investigated by obtaining flux estimates from several spectral lines characteristic of the different important gamma emitting nuclides in the series. We have not yet exploited the possibilities in this area.

Calculations of φ/I

The ratio of flux to exposure rate is the most important quantity needed for determining exposure rates from in situ field spectra. Fortunately some of the problems mentioned in connection with the measurement of source activity for varying depth distributions are not as troublesome when determining exposure rate.

In Table 11 we give values for φ/I for energies of prominent gamma-ray peaks corresponding to the major fallout emitters in the soil. The total exposure rate values were taken from Table 9.

In Figure 4 are plots of φ vs α/ρ, I vs α/ρ, and φ/I vs α/ρ, for 662 keV. The first two quantities vary over a range of almost a factor of 10 between a plane source and a deeply distributed source, but the ratio varies only by 25 - 30%. Thus, even if we have a poor knowledge of the actual depth distribution, our error in field spectrometric estimates of exposure rate is reasonably limited. This is particularly true for deeply distributed radionuclides, i.e. slight deviations of the natural emitters from a completely uniform distribution will not materially effect φ/I. In addition, since the density (water content) enters into both the flux and exposure rate calculations in almost the same manner (see equations 1 - 8), the ratio φ/I is fairly insensitive to the actual density and is almost completely invariant for the uniformly-distributed natural emitters. Similarly, φ/I is also insensitive to the exact soil composition. The values for φ/I are thus of more universal utility when used for interpreting field spectra.

The values of φ/I for the important gamma rays from ^{238}U, and ^{232}Th and ^{40}K are given in Table 12. It should be noted that the values for φ/I given here for the 1.76 MeV ^{214}Bi line or the 2.62 MeV ^{232}Th line differ from the values used in our previous work[5] since both our values for I and for the unscattered flux have been revised. The 1.76 MeV value is only about 10% lower than our previous value and the ^{40}K value changes by only about 5%, although the ^{232}Th value is 20% lower.

The values of φ/I given here may not, of course, be the final ones because uncertainties in some of the photons per disintegration values are still known only to ± 10%. The data in Table 1 - 7, however, allow the reader to revise the tabulated values of φ/I based on any new data or to calculate values for energies and radionuclides not given. Any errors due to differing soil composition and uneven moisture content, even though they may result in quite large errors in the individual values of flux and exposure rate, should not materially affect the ratio.

Importance of Detector Height Above the Interface

All of the quantities above have been calculated for a distance of one meter above the interface in air at 20°C and 760 mm of Hg. It was previously shown that for almost all depth distributions except those approaching a plane source on the surface, the exposure rate and flux vary slowly with height above the interface[12]. Thus one need not correct for changes in air mass due to changing environmental conditions nor is it important that the detector distance be exactly one meter. For example, the flux and exposure rate at one meter due to a ^{137}Cs (662 keV) source distributed in the soil with $\alpha/\rho = 0.63$ are only reduced by 10% and 7%, respectively, from the values at the interface itself. For more uniform source distributions, the decrease with height is even less and the ratios of φ/I are relatively insensitive to the exact detector height.

In real life, the earth-air interface is not a flat plane. This fact manifests itself most significantly when the amplitude of the earth surface undulations become significant

with respect to the detector height. The calculated exposure rates and fluxes then vary from the measured values since in effect the detector "sees" a different amount of source than in the calculational model. Again, the ratio φ/I should be the quantity least affected. Ground roughness may, however, effectively make a surface source appear to be distributed in depth and in fact many investigators simulate ground roughness by a buried plane source. In a real situation, therefore, the detector height could be important if a measurement of flux or total exposure rate alone is being attempted. Our experience indicates that the ratio of φ/I is sufficiently invariant with respect to ground roughness that good results can be obtained for natural emitter exposure rates inferred from flux measurements even over quite poor half-spaces.

Sources Outside the Soil Half-Space

All of the preceding discussion has been for sources in the soil half-space. Field spectrometry is, of course, useful for measuring the gamma rays from other sources, such as noble gases in airborne effluents from nuclear facilities, ^{16}N gamma rays from nuclear power plant turbines employing primary steam from the reactor, other sources of direct radiation from nuclear facilities, and locally contaminated areas. In each case a knowledge of the source geometry is required in order to use the measured flux to infer either source concentration or exposure rate.

These situations are usually difficult to model, as for example the plume of noble gases from a nuclear facility, however, field spectra are useful for identifying the contributors to flux and exposure rate. By utilizing the field spectra to calculate natural and fallout exposure rates and then subtracting these contributions from an ionization chamber measurement of total exposure rate, one can obtain the exposure rate due to the other sources identified in the field spectra.

V. CALIBRATION OF DETECTORS AND ANALYSIS OF SPECTRA

Detector Response to Known Flux (N_o/φ)

The first important requirement for measuring gamma-ray flux is a detector which is accurately calibrated, both as a function of energy (N_o/φ) and as a function of angular incidence (N_f/N_o). Each of the detectors described in Table 13 was calibrated in the laboratory by exposure to known fluxes from standard point sources placed at distances ranging from about 1 - 6 meters from the face of the detector. It is important to place the source as far from the detector as possible in order to simulate a plane beam of incident photons. Corrections must be made for attenuation in the air between the source and the detector and for self-absorption in the source if any. When calibrating the NaI(Tl) detectors, the sources used were chosen to simulate the peaks routinely analyzed in field spectra. For the Ge(Li) detectors, a much more extensive calibration was desired since the increased resolution means one can utilize photopeaks at almost every energy.

Calibration Sources

Many of the standard sources used were obtained from the International Atomic Energy Agency or National Bureau of Standards although a number were standardized here at HASL using beta-gamma coincidence counting. In all cases the beta emission rate of the standards was known to a few percent. For a few sources, uncertainties in gamma emission rate or half-life resulted in uncertainties in the measured N_o/φ greater than ±5%. The use of a large number of sources, and the subsequent fitting of a smooth curve to the data, resulted in what we believe are values of N_o/φ for the Ge(Li) detectors whose accuracy is better than 5% at all energies and better than 2% at energies above 200 keV. The N_o/φ values determined for the NaI(Tl) detectors are somewhat less accurate ($\sim$ 5%) because of the problem of measuring the peak area for a given incident flux.

Determination of Total Absorption Peak Areas

In the case of the Ge(Li) detector calibration, the total absorption peak area obtained due to a given incident flux is determined by fitting the continuum under the peak by an exponential function and then ascribing all the counts above this baseline to the total absorption of incident flux. The calibrations are all carried out by superimposing the source response on top of laboratory background in order to simulate the field situation as closely as possible.

In reality the continuum dominated primarily by Compton scattered gamma rays is not a true exponential. Some investigators fit the peak by assuming it to have a Gaussian shape with a skewed low energy tail. Others fit the continuum by a straight line. We have found by comparing several methods with our method for estimating peak areas, we can determine the actual number of total absorption events within about 2% for our 60 cm^3 Ge(Li) detector and that the more sophisticated techniques do not seem to result in significantly better analyses. For field spectra the statistical counting error for even the strongest peaks is about 5 - 10% for a 30 minute counting interval, and this uncertainty has a greater effect on both the fit to the continuum and the estimate of peak area than the particular method used to fit the continuum.

All of our analyses of Ge(Li) peak areas are done semi-automatically by displaying a portion of the spectrum on a cathode ray screen, instructing a small computer to fit an exponential between two channels indicated by the operator, strip the continuum away and estimate the peak area. The operator can have the computer smooth the data if necessary in order to aid him in determining the end channels for fitting.

The NaI(Tl) peak areas are also estimated by fitting the Compton continuum with an exponential curve as shown in Figure 5. Because of the poorer resolution only very prominent peaks can be resolved, however. As can be seen in the figure which shows a typical field spectrum with fallout present, the 1.46 MeV ^{40}K, 1765 keV ^{214}Bi and 2.62 MeV ^{208}Tl

peaks are quite prominent and their areas can be estimated readily. The fallout peaks are less prominent and the estimates of their areas are considerably less precise.

The calibration of the NaI(Tl) detector for N_0/φ is more difficult than for the Ge(Li) detector since the determination of peak area does not usually account for all the totally absorbed gamma rays (i.e. the exponential fit over the large number of channels encompassed by the typical peak is not an optimum fit). Comparisons of peak areas obtained by subtracting background for monoenergetic calibration source exposures indicate that this method of estimating the continuum results in approximately 20% of the total absorption peak are being missed. However, we found that this percentage is relatively constant among field spectra, because the shape of the NaI continua are relatively constant. This is because the Compton scattered gamma rays from the natural emitters in the soil dominate the NaI(Tl) spectrum and the spectrum is relatively invariant to the amount of K, Th, and U in the soil or to the size of the individual total absorption peaks on the continuum. Thus, if we calibrate the detector in a situation similar to that in the field (i.e. use laboratory background) the absorption peak count fraction we obtain for the calibration is approximately the same as the fraction we obtain in the field for the same incident flux. We can thus obtain a good measure of the in situ flux.

Since this fraction varies somewhat with source energy[1], however, it is mandatory to calibrate for the energies one wishes to measure. The most important criterion here is to be consistent, i.e. to determine peak areas for field spectra in a manner identical to that used for calibration. We were able to do this for all energies except for ^{40}K (1.46 MeV), which is not available as a standard. Here we originally had to rely on calibration measurements using ^{24}Na (1.38 MeV) or ^{42}K (1.58 MeV)[1,6]. A later comparison in the field of the Ge(Li) and NaI(Tl) spectrometers, which will be discussed later, indicated we were able to obtain a reasonably good estimate of N_0/φ for 1.46 MeV.

Another method would be to simulate a source of ^{40}K using KCl or K_2CO_3, measure the flux using the Ge(Li) detector, and then use the measured flux to calibrate the NaI detectors.

Measured Values of N_o/φ

The values obtained for N_o/φ for two 4 in. by 4 in. NaI(Tl) detectors, for the original HASL 25 cm^3 Ge(Li) diode and our present 60 cm^3 diode are given in Tables 14 and 15 along with a description of the calibration sources used. The values for N_o/φ for the large Ge(Li) detector can be represented to within a few percent by the function $\ln(N_o/\varphi) = 4.48 - 1.03 \ln E(MeV)$ over the range 180 keV to 3.0 MeV. Since for the Ge(Li) detector N_o/φ is actually a measure of the total absorption probability, we are justified in drawing a smooth curve and interpolating between energies. This is not justified for NaI(Tl) spectrometry because the N_o/φ values are dependent on the experimenter's method of estimating the continuum.

Table 13 gives pertinent data regarding the construction, efficiency and resolution of each of the detectors calibrated. In all cases the flux referred to is the flux incident on the actual detector at the point of interaction. Note that as long as the source to detector calibration distance is long compared to the distance between the actual point of interaction in the detector and the face of the housing, no significant error results from measuring distances with respect to the housing faces. We determined, by placing sources at various distances from 50 cm to 2 meters from the face of the detector, that the median distance of effective interactions in our 60 cm^3 diode was about 1.6 cm from the housing face. Gamma-ray absorption in the housing is included as part of the detector response.

Note that the values of N_o/φ in Table 14 for the two NaI(Tl) detectors differ by only a few percent from each other, but by about 15% from the values reported for our original 4 in. by 4 in. detectors[5]. This discrepancy indicates that one can be wrong in assuming that two NaI(Tl) detectors of the same nominal size procured at different times, even from the same supplier, will have the same size. The reduction in N_o/φ seemed to be the same for all energies

measured in the present calibration which were not as extensive as that carried out previously, so we merely reduced the N_0/φ data in HASL-170[8] by the appropriate fraction when determining N_0/φ for energies not used in the recalibration.

Angular Response Correction Factor (N_f/N_0)

A complete flux response calibration of the detectors requires a correction factor to account for the fact that the gamma rays incident on the detector in the field situation are not (as shown in Table 6) incident along the axis of symmetry. If $N(\theta)/N_0$ is the ratio of the response to gamma rays of energy E at angle θ with respect to the response at $\theta = 0^\circ$, then

$$N_f/N_0 = \frac{1}{\varphi}\left[\int_0^{\pi/2} \varphi(\theta)\ \frac{N(\theta)}{N_0}\ d\theta\right]. \qquad (10)$$

Fortunately, $N(\theta)$ is nearly unity over all θ for both detectors for all except very low energy gamma rays. This results in values of N_f/N_0 (see Table 16) for the NaI(Tl) peaks of interest most of which are less than 1.1 and in 60 cm^3 Ge(Li) values almost all equal to 1.0 for gamma rays from the soil half space. The angular response of our original 25 cm^3 Ge(Li) detector was more skewed, resulting in larger values of N_f/N_0. The N_f/N_0 ratios were calculated by numerically integrating Equation (10) using a smooth fit to the experimental angular response data to interpolate over $N(\theta)/N_0$. Because the final correction factor is small, errors involved in this interpolation is small. $\varphi(\theta)$ is given by equation (4) in section III.

The angular response of our Ge(Li) detectors is somewhat asymmetrical in the azimuthal direction because of the mounting arrangement, cold finger connection and electrode connections. These deviations from symmetry, however, are quite small except at very low energies (< 100 keV), and involve only a small portion of the total solid angle.

Final Calibration Factors

The final sensitivities of each detector in terms of total absorption peak counts per unit soil activity $N_f = (N_o/\varphi)(N_f/N_o)\varphi$ and peak counts per unit exposure rate $N_f = (N_o/\varphi)(N_f/N_o)(\varphi/I)$ are given in Tables 17 and 18. Note that the 60 cm^3 Ge(Li) detector has an effective sensitivity at lower energies which is greater than its volume ratio to the 25 cm^3 detector would indicate, due to its flatter angular response as well as relatively greater sensitivity at higher energies than at lower energies.

Note also that the final conversion factors for exposure rate vs. source depth distribution vary over a much smaller range than the corresponding factors for soil activity.

Corrections for Interfering Peaks

The values for N_f and N_f/I in Table 18 for certain weak lines such as the 768 keV of ^{214}Bi, the 665 keV ^{214}Bi line, and the 300 keV ^{212}Pb line should not be used as the primary means for determining the flux or exposure rate from the nuclide in question. They do allow a rough estimate of the interference fraction due to a strong peak of the same or very nearly same energy corresponding to a second nuclide. For example, the 766 keV ^{95}Nb peak must be corrected for the 768 keV ^{214}Bi peak, the 662 keV ^{137}Cs for the 665 keV ^{214}Bi peak, etc. We have attempted to include values for all the radium and thorium lines which interfere with important fallout nuclides or with other stronger radium and thorium lines. However, when sources other than those listed are present the investigator should determine any other possible interferences and calculate correction factors based on the data in the Tables in this report.

For the NaI(Tl) detector, the values for the 583 keV ^{208}Tl line and 609 keV ^{214}Bi line are given primarily to allow an estimate of the interference in the broad peak centered approximately around 662 keV when significant amounts of ^{137}Cs are present. A correction factor to the 514 keV ^{106}Ru line is not given since besides the 510 keV

^{208}Tl line there is also a significant contribution from annihilation photons from both cosmic rays and from the pair productions of the higher energy gamma rays in the soil, air and detector housing. Thus, only very large amounts of ^{106}Ru can be readily quantitated with the NaI spectra.

Energy Band Calibration

We have showed that, where only low-energy fallout emitters are present, one could simplify the analyses of NaI(Tl) field spectra for the natural emitters[1,2,5]. A so-called energy band analysis, which is well suited to computer data processing, involves the calculation of the spectrum "energy" (total counts per channel multiplied by the energy represented by that channel) in bands of channels centered on the 1.46 MeV ^{40}K peak, the 1.76 MeV ^{214}Bi peak and the 2.62 MeV ^{208}Tl peak and applies a set of simultaneous equations to calculate these exposure rate contributions. The three equations relating U, Th and K exposure rates to the three band energies were determined by carrying out a regression analysis on a large number of field spectra for which the individual exposure rate values were determined from the peak method. As long as the "energy" in the three chosen bands was due entirely to one or more of the three isotopes and the geometry and source depth distribution were constant, this method worked and proved to give more precise results than the peak method. Because we lacked sufficient field data with our NaI(Tl) detectors to carry out a similar regression analysis, we simply revised the equations given in HASL-170 based on the observed differences in efficiency and our new values for φ/I[5]. The primes on E in the new equations, shown in Table 20, indicate that the energy in each band due to cosmic rays (which is a function of altitude) must be subtracted before applying the equations. The appropriate cosmic-ray correction factors, based on revising the data in HASL-170 for reduced efficiency, are also given in Table 20. The new equations, for the field data obtained so far with the new detectors, give comparable results to the peak method.

Total Spectrum Energy Calibration

The exposure rate in air,

$$I \propto \int_0^\infty \varphi(E)\ \mu_e/\rho\ EdE,$$

where $\varphi(E)$ is the flux of gamma rays of energy E and μ_e/ρ is the mass energy absorption coefficient in air. For energies between a few hundred keV and several MeV μ_e/ρ is fairly constant with energy. Also, for low energies the probability of an incident photon being totally absorbed by a large NaI(Tl) detector is fairly large (on the order of 50 - 100% from 100 keV to ~1 MeV). Most of the exposure rate in air, about 75%, due to emitters in the soil is due to gamma rays between 100 keV and 1.5 MeV[12]. Couple this with the fact that the spectrum of gamma rays from natural emitters is quite invariant to the actual proportions of U, Th and K in the soil[12] and one can see why the total "spectrum energy" is a reasonable measure of free air exposure from natural radioactivity in the soil. In essence the large crystal measures the flux to a fairly high degree of accuracy and, even though it measures a slightly smaller proportion of the flux as the energy increases and some of the secondary scattered energy escapes the detector, this decrease is compensated by correspondingly smaller values of μ_e/ρ at energies above 1 MeV relative to values below 1 MeV.

Unlike many NaI(Tl) instruments, which are based on the assumption that the counting rate above some bias level is proportional to the exposure rate, thus implying that the spectral shape of the gamma-ray field is invariant, this total energy technique requires only that the counts in a channel be proportional to $\varphi(E)(\mu_e/\rho)$ for that energy, and is, therefore, less sensitive to spectral changes. For example, a counter using a large NaI(Tl) detector would record the exposure rate from a unit flux of 60 keV photons as being almost equal to the exposure rate from a unit flux of 1464 keV photons since, even at 1.46 MeV, a pulse would be recorded due to the high probability of a Compton collision in the detector even though many of the secondaries would escape the crystal. In the total energy technique, the higher energy counts are weighted by the energy deposited to reflect more correctly their relative contribution to the exposure rate. The slightly larger total absorption at 60

keV reflects the larger value of (μ_e/ρ) relative to 1500 keV gamma rays.

The total energy technique was tested between 150 keV and 3.4 MeV by comparing the exposure rates determined from our large NaI(Tl) crystals with high pressure ionization chamber measurements for a variety of gamma ray fields. The total energy method results were proportional to exposure rate for various radiation fields varying from low-energy fallout radiation to a predominantly ^{40}K dominated field.

Another advantage in using the NaI detector as a dosimeter is its relative small response to cosmic-ray secondaries over the range of 150 keV to 3.4 MeV. This has allowed us to check independently the cosmic-ray calibrations of our high pressure ionization chambers[6].

We determined the "spectrum energy" calibration factors for our present 4 in. by 4 in. detectors in two ways. First, we exposed the detectors to a known exposure rate from a point ^{226}Ra source in the laboratory as determined by an ionization chamber measurement. This measurement was corrected to account for the fact that the gamma rays in the laboratory were incident along the detector axis. The angular correction factor (1.11) was estimated by folding in our previous calculations of the angular exposure rate distribution for a field situation[12] with the measured response of "spectrum energy" as a function of the angle of incidence.

The second method of determining the proportionality factor was to compare measurements of "spectrum energy" for actual field spectra with simultaneous ionization chamber measurements over a range of fields. The two methods gave essentially the same calibration factors. We noted again that these factors were about 85% of the values obtained for our previous 4 in. by 4 in. detectors. These total "energy" to exposure rate conversion factors are given in Table 20, along with the appropriate cosmic-ray correction factors.

One further point regarding the use of "spectrum energy" technique is that although at h = 1 meter about 40% of the

gamma ray flux is below 150 keV this flux (about half of which is due to skyshine) accounts for less than 10% of the exposure rate[12,22]. Thus, integrating from 150 keV up does not introduce serious error into exposure rate estimates, however, a count rate meter biased below 150 keV will be sensitive to changes in low energy flux and, because of the large fraction of "skyshine", will be quite angularly dependent.

Summary of Calibrations and Analyses

Because of the length and complexity of the preceeding discussion it may be valuable to summarize the use of field spectrometry to determine source activity or exposure rates from particular nuclides in the soil:

1. Determine the response of the detector to a known flux of gamma rays of energy E, incident along the detector axis, where E is the energy of a prominent gamma-ray transition characteristic of the source. (N_0/φ - Tables 14, 15).

2. Using equations (3) or (4) for the angular incidence of gamma rays on the detector for given source depth distributions, determine the correction to be made to N_0/φ. (N_f/N_0 - Table 16).

3. If the source is one for which we have already calculated the flux φ, for the gamma-ray energy of interest (Table 3 or 4), and the exposure I (Table 8 or 9), multiply each of these values by N_0/φ and N_f/N_0 to obtain the required calibration factor.

4. If the nuclide and source distribution is one for which we have not determined φ and I, use the data in Table 1 or interpolations thereof and appropriate values of photons per disintegration to determine φ. Using the data in Table 7, or interpolations thereof, sum over all the gamma-ray transitions for a given nuclide to determine I for that source for a depth distribution of interest.

5. Finally, to determine the source activity or exposure rate from a specific radionuclide, estimate the peak area in the field spectrum in a manner identical to that used

during the calibration, subtract any counts in the peak due to the same energy transitions from other nuclides (see "Corrections for Interfering Peaks", page 24), and then divide by the appropriate calibration factor to obtain the desired activity or the exposure rate.

VI. APPLICATIONS OF FIELD SPECTROMETRY

Typical Field Spectra

Figure 6 shows a NaI(Tl) field spectrum obtained at a location in the Northeastern United States. Figure 7 shows the Ge(Li) spectrum obtained with the 60 cm^3 Ge(Li) detector simultaneously at the same site. The Ge(Li) spectrum represents a 30 - 40 minute measurement and the NaI(Tl) spectrum, 20 minutes. The former spectrum conveys far more information even though the efficiency of the detector is lower. For example, one can measure fluxes at several dozen energies, including that due to ^{144}Ce (134 keV) and ^{126}Sb (428 keV) which are not identifiable in the NaI(Tl) spectrum. In addition, the important ^{137}Cs peak is completely resolved instead of being partially combined with an array of Th and U peaks.

Examples of Field Spectrometric Results

Table 21 gives some individual nuclide exposure rates calculated from spectra for a variety of environmental radiation fields and compared with independent ionization chamber measurements. Even the NaI(Tl) spectrometer is a powerful tool, as is shown, for example by the data obtained at Bikini Atoll for a pure fallout field. Comparing exposure rates at a number of the sites illustrates that both methods give comparable exposure rate results for the natural emitters and major fallout nuclides, and as expected the Ge(Li) detector is more useful for analyzing more complex fields. The relative accuracy of the spectrometric analysis methods described earlier is indicated in the table by the degree to which the

sum of the individual nuclide exposure rates add up to the total (ionization chamber) measured exposure rate over a wide range of radiation fields.

Determining Source Radioactive Equilibrium

The statistical precision of the flux measured from a single major peak is less precise for a Ge(Li) than for a NaI(Tl) spectrum. We can, however, measure the flux from several lines for say the ^{238}U or ^{232}Th series and obtain a more precise measurement of the exposure rate from the whole series. In the case of the ^{232}Th series, one can ascertain the degree of equilibrium among various nuclides in the series (particularly the degree of equilibrium between $MsTh_2$ and its daughters since ^{224}Ra may be leached out of some soils and between ^{226}Ra (186 keV) and radon daughters).

Nuclear Facilities Studies

In addition to measuring exposure rates and concentrations of natural emitters and deposited fallout emitters, field spectrometry is also quite valuable for investigating the radiation field around nuclear facilities. Even when a nuclear facility is operating, the natural background and fallout exposure rate levels can be unambiguously distinguished by Ge(Li) field spectrometry from the exposure rate contributions from other sources, such as effluent noble gases and direct radiation from waste storage and steam turbines.

Figure 8 shows Ge(Li) spectra obtained at a site near a boiling water reactor (BWR) nuclear plant with the wind blowing from the BWR stack toward the detector and in the opposite direction. The peaks due to the noble gases can be clearly identified and the fluxes of these gamma rays at the detector estimated. For accurate measurements, however, we need to know the geometry of the plume in order to relate fluxes at the indicated energies to exposure rates from the individual nuclides. We can, however, test models of plume geometry by using the ratios of fluxes at the detector due to different gamma-ray energy lines from the same nuclide, for example the 403 keV to 2556 keV ^{87}Kr lines or the 196 to 2196 keV ^{88}Kr lines. The total plume exposure rate can, of course,

be easily obtained by subtracting the spectrometrically determined natural and fallout components from the total exposure rate determined with the ionization chamber.

The Ge(Li) spectrum can be used to quantitate the exposure rates or concentrations of any nuclides deposited on the ground, such as ^{131}I or ^{134}Cs, using the usual techniques. An example of a situation which could be analyzed semi-quantitatively is shown in Figure 9, a Ge(Li) spectrum obtained along a river bank near a nuclear fuel reprocessing plant. Here the clay apparently filtered and concentrated certain nuclides present in the water (particularly cesium), resulting in a substantial increase in local environmental radiation levels.

^{16}N from BWR Turbines

Another application of field spectrometry is the measurement of the flux and exposure rate in the environment due to the high energy gamma rays from ^{16}N in the steam passing through the turbines of large BWR plants (Figure 10). Here the high sensitivity of NaI(Tl) even at these higher gamma-ray energies provided a sensitive indication of the presence of higher energy gamma rays, particularly since there are no natural or fallout emitted gamma rays above 3.0 MeV. Using the measured flux and the total spectrum energy above 3 MeV Lowder[23] has shown that quite accurate estimates of ^{16}N environmental exposure rates can be made.

Radioactive Construction Materials

We have also used *in situ* spectrometry to qualitatively identify the presence of low energy gamma rays from radium present in uranium tailings used for building construction and to identify the source of elevated exposure rate levels in structures built using high phosphate material or certain types of uranium bearing shale.

^{239}Pu in the Environment

Field spectrometry can also be used to monitor special radiation contamination situations such as deposited ^{239}Pu

in the soil surface. Here, large area, thin NaI(Tl) detectors are used to monitor the 60 keV ^{241}Am gamma rays which accompany ^{239}Pu. Our laboratory studies of the response of our large 60 cm^3 Ge(Li) at 60 keV indicate that one could identify elevated levels of ^{239}Pu in the environment. Though systematic studies have not been made, one notes that a large fraction of the low energy flux contributing to the Compton continuum in the 60 keV energy region is due to "skyshine" and, therefore, the "background" in this region can probably be dramatically reduced by judicious shielding and the ability to measure the 60 keV line enhanced.

Estimates of Soil ^{90}Sr and ^{137}Cs Levels

Finally, field spectrometry is useful for rapid determinations of the variation of fallout within some geographical area. Here, as mentioned previously, we need to know the depth distribution of radioactivity fairly accurately to arrive at a very accurate concentration measurement, though one can still obtain a picture of the gross variation with location. For example, Table 22 shows estimates of ^{137}Cs activity in soil in the mid 1960's made by measuring the 662 keV flux at 1 meter above the ground, assuming that a 3 cm relaxation length represents the mean depth distribution (α/ρ = 0.21, at that time was a reasonable value based on the few available measurements) and the empirically accepted fact that the ^{90}Sr/^{137}Cs activity is about 1.5[24]. Estimates from field spectrometry can be seen to compare well with the soil sample results of Hardy and Alexander[24]. The fact that one can estimate the gross activity of ^{137}Cs or ^{90}Sr at a site to even an accuracy of a factor of two (if the assumed depth distribution was wrong) seems significant in the light of the speed with which the spectral measurements can be made.

Relative Advantages of NaI(Tl) and Ge(Li) Systems

Although Ge(Li) spectra clearly give much more information than the NaI(Tl) spectra, to gather and utilize this information requires a large capacity multichannel analyzer having 1000 or more channels, a separate amplifier, liquid nitrogen supply and readout equipment to store the large amount of data. One also obtains much more data for analysis than may

be needed for a particular problem. Conversely the NaI(Tl) detector requires only a 200 - 400 channel analyzer and a parallel printer. Power requirements can be met with only one 12 V storage battery and a small rotary inverter. One can operate the equipment required for a NaI(Tl) field spectrum out of the trunk of a standard auto. For most "natural background" measurements, it is clear from the data in the preceding tables that the NaI analysis is completely adequate.

Though the cost of the Ge(Li) system is quite high, its utility is obvious for investigating complex radiation fields. The proper mounting in a station wagon or panel truck allows the spectrometer to be easily transported and allows maximum utilization both as a field spectrometer and as a standard laboratory counting system.

VII. ESTIMATES OF ERRORS IN THE DETERMINATION OF FLUX, EXPOSURE RATE AND SOIL ACTIVITY

We have tried to indicate at each step the necessary approximations and possible sources of error. It is clear that the final assessment of the accuracy of the method must rely on (1) cross-calibrations by other techniques of analysis and (2) the degree by which the sum of the individual exposure rates agrees with independently measured total exposure rates over a wide range of K, Th, U and fallout combinations.

We previously showed that the use of NaI(Tl) spectrometry to measure the soil activity of U, T and K was quite accurate having tested the assumptions of half-space geometry, uniformly distributed sources, insensitivity to soil density, etc. by comparing field spectrometric estimates of <u>in situ</u> soil activity with laboratory analyses of soil samples taken at a large number of sites[1]. For both K and Th our estimates of concentration correlated very closely with the laboratory estimates, although the field estimates were in general about 10% lower than the laboratory results. This was expected, however, since the latter were concentrations in dry soil and

an average increase of 10% in soil density due to in situ moisture content appeared reasonable. Individual comparisons in some cases showed poorer agreement and this probably reflected more the problem of obtaining a representative soil sample at a site than an error in the field spectral analysis. The U series comparison was, of course, very poor reflecting primarily the different radon emanation fractions at the various sites, since most of the soils were counted in the laboratory after being allowed to reach equilibrium. A few samples which were counted in the lab after drying and before being allowed to reach equilibrium indicated losses of from 30% to 50% of the radium equivalent gamma activity.

In the previous section we compared our field spectrometric estimates of ^{137}Cs and ^{90}Sr measurements on laboratory samples, indicating in general very good agreement.

Table 21 indicated the degree to which the individual exposure rate estimates sum to the total ionization chamber value of exposure rate. These data are in general accord with our experience at most reasonably flat "half space" sites and are the best indication of the validity of our individual exposure rate estimates.

In general, the largest percentage error in exposure rate is obtained for the ^{238}U series, primarily because of the emanation of radon and its subsequent movement within the atmosphere. Besides resulting in a somewhat altered source distribution with respect to our model, the decreased flux results in poorer quality counting data. For example, it is frequently quite difficult to accurately estimate the small flux of 1.76 MeV gamma rays present from NaI(Tl) spectral data. Combining the accuracy of flux estimation (± 20%) with the uncertainty in radon contribution we estimate our ^{238}U series exposure rate values are correct to about 25%. Because of the ability to resolve the 295, 350, and 609 keV U peaks with the Ge(Li) detector we are able to obtain much better measurements of flux (~ ± 5% s.d.) and we estimate our Ge(Li) ^{238}U exposure rate measurements to have an accuracy of ± 10 to 15%. In terms of the error in total exposure rate this percentage is small since generally ^{238}U contributes only

about 20% to the total gamma exposure rate. The ^{40}K estimates are the most accurate and we feel our measurements of flux are good to better than 5% and our estimates of exposure rate to about 5 - 10%. Thorium-232 exposure rates are also believed to be correct to about 5 - 10%.

The error in estimating fallout soil activities has already been shown to be dominated by the accuracy of the assumed depth distribution. We estimate we can infer ^{137}Cs exposure rates to ± 15% with the NaI(Tl) detector and ± 10% with the Ge(Li) under most circumstances.

These are accuracy estimates and include systematic errors such as uncertainties in branching ratios. The precision of a single measurement depends on the statistical significance of the counting rate data under the photopeaks of interest. For prominent peaks such as the 1464 keV ^{40}K peak the precision can be better than the accuracy, i.e. we can reproduce the measurement to better than a few percent although the actual error in our estimate of exposure rate may be much greater. Thus, it is quite feasible to use the spectrometric technique to study small time variations in background due to changes in soil moisture, radon emanation, and "natural fallout".

VIII. SUMMARY

We have attempted in this report to summarize all of our work to date on <u>in situ</u> field spectrometry, presenting in detail the theoretical basis for interpreting field spectra to determine soil concentrations and exposure rates as well as illustrating the laboratory calibration of our particular detectors. In doing so we have tried to indicate the "detector independence" of the method, pointing out that the detector can be any instrument which measures the gamma-ray fluxes at particular energies.

We have pointed out the use of particular field spectrometric systems for investigating various environmental radiation fields, both natural and man-made. Field spectrometry is a powerful tool for studying external environmental radioactivity. It allows one to obtain quantitative data over large areas in a short time, a task that is clearly impractical by conventional sample gathering and subsequent laboratory analysis. It also allows one to pick and choose sites for further or for more intensive study, provides at the very least qualitative information on the sources contributing to the gamma-ray exposure at a site and at its best a complete quantiative picture of the gamma-ray field.

We have attempted to include in this report the theoretical data necessary to infer soil activity and free air exposure rate for any source whose depth distribution in the soil can be represented by a superposition of exponentials and whose energy lies between 50 keV and 3 MeV. Thus, it would be an easy matter for instance for any investigator to use the tables in this report to estimate the flux at 1 meter above the ground due for example to a quasi-plane source of ^{134}Cs or ^{60}Co or any other similarly unlikely contamination situations.

All of the data in this report refer to measurements to be made at or near the earth-air interface. Clearly there are similar possibilities for field spectrometry from aircraft. We previously discussed the variation of exposure rate and flux with altitude[12] and these data can be used to infer appropriate values of φ/I above the ground. The theoretical results are being modified as necessary to reflect the more accurate data for photons per disintegration in the ^{238}U and ^{232}Th series, as well as to provide energy and angular distributions for photon flux as well as for exposure rate as a function of altitude.

ACKNOWLEDGMENTS

The authors wish to acknowledge the considerable contributions to this work by several of our HASL colleagues, in particular, Peter Raft, Wayne Lowder, Burton Bennett, and James E. McLaughlin. We wish to particularly thank the HASL Instrumentation group for their help in the design, procurement, and construction of the instrument systems described in this report.

REFERENCES

1. Beck, H. L., Condon, W. J., and Lowder, W. M.
   Spectrometric Techniques for Measuring Environmental Gamma Radiation
   USAEC Report HASL-150, October (1964)

2. Lowder, W. M., Condon, W. J., and Beck, H. L.
   Field Spectrometric Investigations of Environmental Radiation in the U.S.A.
   The Natural Radiation Environment, Ch. 35 (Adams, J.A.S., Lowder, W. M., Editors)
   Univ. of Chicago Press, Chicago (1964)

3. Beck, H. L., Lowder, W. M., and McLaughlin, J. E.
   In Situ External Environmental Gamma-Ray Measurements Utilizing Ge(Li) and NaI(Tl) Spectrometry and Pressurized Ionization Chambers
   Proc. of Symposium on Rapid Methods for Measuring Radioactivity in the Environment
   IAEA-SM-148/2, Vienna (1971)

4. Lowder, W. M., Beck, H. L., and Condon, W. J.
   Spectrometric Determination of Dose Rates from Natural and Fallout Gamma-Radiation in the United States, 1962 - 1963
   Nature, 202, 745-749 (1964)

5. Beck, H. L., Lowder, W. M., Bennett, B. G., and Condon, W. J.
   Further Studies of External Environmental Radiation
   USAEC Report HASL-170, March (1966)

6. Moriuchi, S., and Miyanaga, I.
   A Spectrometric Method for Measurement of Low-Level Gamma Exposure Dose
   Health Physics, 12, 541 (1966)

7. Pensko, J.
Dosimetry of Environmental Gamma Radiation in Poland by Means of Gamma-Ray Spectra in the Field
Central Laboratory for Radiological Protection Report CLOR-48/D, Warsaw (1966)

8. Cardinale, A., and Frittelli, L.
Improved Methods for the Measurement of Gamma Exposure Rate in the Natural Radiation Environment
Comitato Nazionale Energia Nucleare Report RT/FI(68)54, Rome (1968)

9. Phelps, P. L., Anspaugh, L. R., Koranda, J. J., and Huckabay, G. W.
A Portable Ge(Li) Detector for Field Measurement of Radionuclides in the Environment
IEEE Transactions on Nuclear Science 1972 (in press)

10. DeCampo, J., Beck, H. L., and Raft, P., High Pressure Ionization Chambers for the Measurement of Environmental Exposure Rates
USAEC Report HASL-260 (1972)

11. Beck, H. L.
Environmental Gamma Radiation from Deposited Fission Products, 1960 - 1964
Health Physics, 12, 313-322 (1966)

12. Beck, H. L., and De Planque, G.
The Radiation Field in Air Due to Distributed Gamma-Ray Sources in the Ground
USAEC Report HASL-195, May (1968)

13. Martin, M. J., and Blichert-Toft, P. H.
Radioactive Atoms
Nuclear Data Tables, Section A, Vol. 8, Nos. 1-2, October (1970)

14. Gunnink, R., Niday, J. B., Anderson, R. P., and Meyer, R. A.
Gamma-Ray Energies and Intensities
LRL Report UC10-15439 (1969)

15. Lingeman, E. W. A., Konijn, J., Polak, P., and Wapstra, A. H.
The Decay of ^{214}Pb and other ^{226}Ra Daughters
Nuclear Physics, A 133, 630-647 (1969)

16. Mowatt, R. S.
^{152}Eu and ^{226}Ra Relative γ-Ray Intensities for Rapid Efficiency Calibrations of Ge(Li) Detectors
Canadian Journal of Physics, 48, 2606-2608 (1970)

17. Maria, H., Ythier, C., Ardison, G., Dalmasso, J., and Forest, H., Compt. Rend., Ser. B., Vol. 265, pp. 1138-40 (1967); Vol. 267, pp. 1109-1112, (1968); Vol. 269, pp. 785-788, (1969); Vol. 269, pp. 1003-1006 (1969); Vol. 272, pp. 905-908 (1971)

18. Beck, H. L.
The Absolute Intensities of Gamma Rays from the Decay of ^{238}U and ^{232}Th (to be published)

19. Hultquist, B.
Studies of Naturally Occurring Ionizing Radiations, with Special Reference to Radiation Doses in Swedish Houses of Various Types
Kungl. Svenska Vetenskapsakad. Handl. 6 Ser. 4, No. 3, p. 125 (1956)

20. Baranov, V. L., as quoted in Grammokov, A. B.
Field Emanation Method, Radiometric Methods in the Prospecting of Uranium Ores, Moscow: State Scientific-Technical Publishers of Literature of Geology and Mineral Resources Conservation (1957) [In English Transl. USAEC Report AEC-tr-3738 (1959)]

21. Vinogradov, A. P.
The Geochemistry of Rare and Dispersed Chemical Elements in Soils, Ch. 16, 2nd ed., p. 212 (1959) [Translated from Russian:New York:Consultants Bureau, p. 212 (1959)]

22. Beck, H. L.
The Physics of Environmental Radiation Fields
Proceedings of the 2nd International Symposium on the Natural Radiation Environment, Houston, Texas (1972) [in press]

23. Lowder, W. M., Raft, P. D., and Gogolak, C. V.
Environmental Gamma Radiation from N-16 in Reactor Turbines
Transactions of the American Nuclear Society, 15, June (1972)

24. Hardy, E., Private Communication (1971)

TABLE 1

φ - UNSCATTERED FLUX AT ONE METER ABOVE GROUND FOR EXPONENTIALLY DISTRIBUTED SOURCES IN THE SOIL*

Source Energy (keV)	(α/ρ)-cm^2/g						
	0 (Uniform)	0.0625	0.206	0.312	0.625	6.25	∞ (Plane)
50	1.4403	0.0816	0.2245	0.3049	0.4748	1.147	1.577
100	2.7744	0.1458	0.3627	0.4708	0.6786	1.359	1.710
150	3.3264	0.1702	0.4103	0.5261	0.7438	1.427	1.775
200	3.9056	0.1843	0.4550	0.5770	0.8018	1.483	1.804
250	4.0640	0.2008	0.4697	0.5910	0.8185	1.506	1.863
364	4.7184	0.2268	0.5158	0.6429	0.8775	1.578	1.933
500	5.3904	0.2519	0.5595	0.6918	0.9334	1.650	1.995
662	6.1456	0.2788	0.6041	0.7412	0.9889	1.719	2.054
750	6.5312	0.2919	0.6257	0.7649	1.015	1.752	2.084
1000	7.5280	0.3245	0.6769	0.8209	1.077	1.830	2.151
1173	8.1472	0.3437	0.7067	0.8531	1.113	1.874	2.189
1250	8.4384	0.3523	0.7198	0.8675	1.129	1.895	2.205
1333	8.7504	0.3617	0.7336	0.8826	1.145	1.914	2.224
1460	9.1472	0.3731	0.7511	0.9011	1.166	1.941	2.247
1765	10.091	0.3997	0.7897	0.9428	1.211	1.997	2.294
2004	10.818	0.4188	0.8173	0.9725	1.243	2.036	2.334
2250	11.397	0.4357	0.8414	0.9982	1.271	2.071	2.358
2500	12.173	0.4536	0.8667	1.025	1.300	2.105	2.385

*The activity at depth Z cm or ρZ g/cm^2 is S(gammas emitted per gram soil per sec) = α/ρ S_A $e^{-(\alpha/\rho)(\rho Z)}$ where S_A = 1.0 gamma/cm^2-s is the total number of gammas emitted in a column of area 1 cm^2 and infinite depth (see equation 3). For α/ρ = 0, S_o/ρ = 1.0 gammas emitted per gram of soil for all Z.

TABLE 2

MASS ATTENUATION COEFFICIENTS IN SOILS OF VARYING MOISTURE CONTENT AND COMPOSITION OF SOIL USED IN TRANSPORT CALCULATIONS

	(μ/ρ) - cm^2/g				
E(keV)	Soil 0% H_2O	Soil 10% H_2O	Soil 25% H_2O	Alum.	Air
20	3.01	2.78	2.05	3.22	0.683
25	2.34	1.52	1.13	1.76	-
30	1.00	0.938	0.838	1.03	0.315
35	0.656	0.644	0.566	0.669	-
40	0.470	0.471	0.433	0.492	0.225
45	0.380	0.381	0.338	0.386	-
50	0.327	0.314	0.298	0.319	0.193
55	0.282	0.277	0.265	0.277	-
60	0.254	0.248	0.239	0.246	0.177
65	0.233	0.230	0.221	0.219	-
70	0.218	0.214	0.206	0.205	-
75	0.204	0.202	0.194	0.193	-
80	0.192	0.190	0.189	0.185	0.161
85	0.189	0.185	0.181	0.177	-
90	0.179	0.178	0.175	0.171	-
95	0.173	0.173	0.170	0.166	-
100	0.166	0.167	0.167	0.160	0.151
150	0.138	0.139	0.141	0.134	0.134
200	0.124	0.125	0.127	0.120	0.123
250	0.114	0.115	0.118	0.111	-
300	0.106	0.108	0.109	0.103	0.106
350	0.100	0.101	0.105	0.098	-
400	0.0950	0.0963	0.0975	0.0925	0.0953
450	0.0906	0.0919	0.0931	0.0875	-
500	0.0869	0.0875	0.0894	0.0844	0.0868
550	0.0831	0.0844	0.0856	0.0806	-
600	0.0800	0.0813	0.0825	0.0775	0.0804
650	0.0769	0.0788	0.0800	0.0756	-
700	0.0744	0.0756	0.0775	0.0731	-
750	0.0725	0.0731	0.0750	0.0706	-

TABLE 2 (Cont'd)

	(μ/ρ) - cm^2/g				
E (keV)	Soil 0% H_2O	Soil 10% H_2O	Soil 25% H_2O	Alum.	Air
750	0.0725	0.0731	0.0750	0.0706	-
800	0.0706	0.0713	0.0725	0.0681	0.0706
850	0.0681	0.0694	0.0706	0.0669	-
900	0.0669	0.0675	0.0688	0.0644	-
950	0.0656	0.0650	0.0669	0.0631	-
1000	0.0638	0.0638	0.0650	0.0614	0.0635
1500	0.0515	0.0521	0.0530	0.0500	0.0517
2000	0.0444	0.0449	0.0456	0.0432	0.0444
2500	0.0398	0.0401	0.0413	0.0388	-
3000	0.0362	0.0364	0.0371	0.0353	0.0358

Composition by weight of soil used in transport calculations:

Al_2O_3 - 13.5%

Fe_2O_3 - 4.5%

SiO_2 - 67.5%

CO_2 - 4.5%

H_2O - 10%

TABLE 3

φ - UNSCATTERED FLUX PER mCi/km^2 AT ONE METER ABOVE GROUND FOR TYPICAL FALLOUT ISOTOPES IN THE SOIL

Isotope	E_γ(keV)	γ's/dis.	(α/ρ) - cm^2/g					
			0.0625	0.206	0.312	0.625	6.25	∞ (Plane)
^{144}Ce	134	.108	6.51(-5)	1.59(-4)	2.04(-4)	2.90(-4)	5.63(-4)	6.99(-4)
^{141}Ce	145	.490	3.03(-4)	7.43(-4)	9.43(-4)	1.34(-3)	2.57(-3)	3.21(-3)
^{131}I	364	.824	6.92(-4)	1.58(-3)	1.96(-3)	2.67(-3)	4.82(-3)	5.88(-3)
^{125}Sb	428	.296	2.63(-4)	5.89(-4)	7.39(-4)	9.88(-4)	1.75(-3)	2.15(-3)
^{140}La	487	.45	4.13(-4)	9.19(-4)	1.14(-3)	1.54(-3)	2.71(-3)	3.30(-3)
^{103}Ru	497	.89	8.20(-4)	1.84(-3)	2.27(-3)	3.08(-3)	5.43(-3)	6.59(-3)
^{106}Ru	512	.206	1.94(-4)	4.34(-4)	5.33(-4)	7.16(-4)	1.27(-3)	1.53(-3)
^{140}Ba	537	.238	2.29(-4)	5.11(-4)	6.25(-4)	8.37(-4)	1.47(-3)	1.78(-3)
^{126}Sb	601	.184	1.84(-4)	4.02(-4)	4.90(-4)	6.57(-4)	1.14(-3)	1.38(-3)
^{105}Ru	610	.054	5.33(-5)	1.18(-4)	1.44(-4)	1.93(-4)	3.40(-4)	4.06(-4)
^{106}Ru	622	.10	1.00(-4)	2.19(-4)	2.68(-4)	3.59(-4)	6.29(-4)	7.55(-4)
^{137}Cs	662	.846	8.73(-4)	1.89(-3)	2.32(-3)	3.08(-3)	5.38(-3)	6.42(-3)
^{95}Zr	724	.435	4.67(-4)	9.98(-4)	1.22(-3)	1.61(-3)	2.82(-3)	3.33(-3)
^{95}Zr	757	.543	5.91(-4)	1.27(-3)	1.54(-3)	2.07(-3)	3.54(-3)	4.22(-3)
^{95}Nb	766	.998	1.09(-3)	2.35(-3)	2.85(-3)	3.85(-3)	6.59(-3)	7.77(-3)
^{140}La	816	.231	2.58(-4)	5.47(-4)	6.67(-4)	8.97(-4)	1.54(-3)	1.81(-3)
^{54}Mn	835	1.0	1.13(-3)	2.39(-3)	2.89(-3)	3.89(-3)	6.66(-3)	7.84(-3)
^{140}La	1597	.956	1.38(-3)	2.71(-3)	3.26(-3)	4.21(-3)	6.93(-3)	8.03(-3)
^{60}Co	1173	1.0	1.27(-3)	2.62(-3)	3.16(-3)	4.12(-3)	6.93(-3)	8.10(-3)
^{60}Co	1333	1.0	1.34(-3)	2.72(-3)	3.27(-3)	4.24(-3)	7.08(-3)	8.23(-3)

TABLE 4

φ - UNSCATTERED FLUX PER pCi/g AT ONE METER ABOVE GROUND FOR UNIFORMLY DISTRIBUTED ^{238}Ra AND ^{232}Th SOURCES IN THE SOIL

Decaying Isotope	E(keV)	γ's/dis.*	Flux (γ's/cm^2-s)	Decaying Isotope	E(keV)	γ's/dis.*	Flux (γ's/cm^2-s)
^{226}Ra	186	0.034	4.58(-3)	^{212}Pb	239 }	0.490	7.25(-2)
^{214}Pb	242	0.070	1.04(-2)	^{224}Ra	241 }		
|	295	0.179	2.91(-2)	^{228}Ac	270 }	0.065	1.02(-2)
|	352	0.350	6.01(-2)	^{208}Tl	277 }		
^{214}Bi	609	0.430	9.42(-2)	^{228}Ac	282		
|	666	0.015	3.39(-3)	^{212}Pb	301	0.034	5.53(-3)
|	768	0.048	1.17(-2)	^{228}Ac	338	0.129	2.18(-2)
|	934	0.031	8.10(-3)	Mixed	328-340	0.172	2.90(-2)
|	1120	0.145	4.21(-2)	^{228}Ac	463	0.047	9.20(-3)
|	1238	0.056	1.72(-2)	^{208}Tl	510	0.096	1.93(-2)
|	1378	0.046	1.49(-2)	^{208}Tl	583	0.300	6.39(-2)
|	1401-08	0.038	1.25(-2)	^{212}Bi, ^{228}Ac	727	0.079	1.86(-2)
|	1510	0.021	7.12(-3)	^{228}Ac	755	0.011	2.70(-3)
|	1730	0.028	1.02(-2)	|	772	0.017	4.10(-3)
|	1765	0.147	5.39(-2)	|	795	0.049	1.20(-2)
|	1848	0.021	7.91(-3)	|	830+35+40	0.038	9.40(-3)
|	2205	0.047	1.95(-2)	^{208}Tl	860	0.047	1.18(-2)
|	2448	0.015	6.66(-3)	^{228}Ac	911	0.290	7.55(-2)
^{228}Ac	129	0.025	2.90(-3)	|	965+69	0.230	6.13(-2)
	210	0.041	5.80(-3)	|	1588	0.046	1.23(-2)
				^{208}Tl	2615	0.360	0.167

*Transitions for which γ's/dis. <.02 are not listed except where they are required to correct measurements of the flux from some other natural or fallout emitter. Series equilibrium is assumed.

TABLE 5

^{238}U, ^{40}K, AND ^{232}Th DECAY CHAINS

Isotope	Decay Mode	$T_{\frac{1}{2}}$	Isotope	Decay Mode	$T_{\frac{1}{2}}$
^{232}Th	α	1.40(10)y	^{238}U(UI)	α	4.5(9)y
↓			↓		
^{228}Ra(MsI)	β-	6.7 y	^{234}Th(UXI)	β-	24.1 d
↓			↓		
^{228}Ac(MsII)	β-	6.13 h	^{234m}Pa(UXII)	β-	1.18 m
↓			↓		
^{228}Th	α	1.91 y	^{234}U(UII)	α	2.5(5)y
↓			↓		
^{224}Ra(ThX)	α	3.64 d	^{230}Th(I_o)	α	8(4)y
↓			↓		
^{220}Rn(thoron)	α	54.5 s	^{226}Ra	α	1622 y
↓			↓		
^{216}Po(Th-A)	α	0.16 s	^{222}Rn(radon)	α	3.83 d
↓			↓		
^{212}Pb(Th-B)	β-	10.64 h	^{218}Po(RaA)	α(99.97%)	3.05 m
↓			↓		
^{212}Bi(Th-C)	α(36%)	60.5 m	^{214}Pb(RaB)	β-	26.8 m
↓	β-(64%)		↓		
^{212}Po(Th-C′)	α	3(-7)s	^{214}Bi(RaC)	β-(99%)	19.7 m
^{208}Tl(Th-C″)	β-	3.1 m	↓		
↓			^{214}Po(RaC′)	α	1.6(-4)s
^{208}Pb	Stable		↓		
			^{210}Tl(RaC″)	β-	1.5 m
			↓		
^{40}K ⎤	10.7% e_K	1.28(9)y	^{210}Pb(RaD)	β-	22 y
↓	89.3% β-		↓		
^{40}A ⎥ β-	Stable		^{210}Bi(RaE)	β-	5.02 d
^{40}Ca ⎦	Stable		↓		
			^{210}Po	α	1383 d
			↓		
			^{206}Pb	Stable	

TABLE 6

PERCENT OF UNSCATTERED FLUX ENTERING DETECTOR AT ANGLES LESS THAN θ FOR h = 1 METER

θ (deg.)	Tan θ=R (meters)	145 keV			662 keV			1460 keV		
		α/ρ=0,	=0.21,	=∞	α/ρ=0,	=0.21,	=∞	α/ρ=0,	=0.21,	=∞
90	∞	100	100	100	100	100	100	100	100	100
84	9.95	93	89	62	92	85	53	92	83	51
79	4.90	84	76	45	82	70	39	82	67	36
73	3.18	73	64	34	72	58	30	72	54	27
66	2.29	63	52	26	62	46	23	61	43	21
60	1.73	53	42	20	52	37	17	52	33	16
53	1.33	43	32	15	41	28	13	41	25	11
46	1.02	32	23	10	31	20	9	31	18	8
37	0.75	21	15	6	21	13	6	21	11	5
26	0.48	11	7	3	10	6	3	10	5	2

Note: θ is measured with respect to the normal to the interface, i.e., θ = 90° is parallel to the interface.

TABLE 7

EXPOSURE RATE (μR/hr) AT ONE METER ABOVE GROUND FOR EXPONENTIALLY DISTRIBUTED MONOENERGETIC SOURCES IN THE SOIL*

Source Energy (keV)	(α/ρ)-cm^2/g						
	0 (Uniform)	0.0625	0.206	0.312	0.625	6.25	∞ (Plane)
50	0.88	-	-	-	-	-	-
100	2.05	~0.095	0.185	0.215	0.270	0.400	0.438
150	3.39	0.140	0.285	0.335	0.418	0.620	0.700
200	4.88	0.200	0.390	0.460	0.570	0.845	0.960
250	6.37	0.258	0.491	0.583	0.731	1.08	1.25
364	10.2	0.404	0.771	0.896	1.11	1.63	1.91
500	14.4	0.558	1.03	1.23	1.52	2.27	2.60
662	19.6	0.738	1.37	1.60	1.97	2.95	3.39
750	22.6	0.837	1.54	1.80	2.21	3.32	3.80
1000	30.4	1.10	2.00	2.32	2.85	4.28	4.86
1173	36.2	1.28	2.31	2.63	3.27	4.87	5.52
1250	38.4	1.33	2.41	2.79	3.42	5.14	5.86
1333	41.8	1.42	2.56	2.95	3.62	5.35	6.16
1460	45.1	1.54	2.75	3.18	3.88	5.73	6.56
1765	54.6	1.78	3.25	3.75	4.40	6.45	7.78
2004	62.2	2.07	3.60	4.13	5.00	7.15	8.20
2250	69.5	-	-	-	-	-	-
2500	77.2	-	-	-	-	-	-
2750	85.0	-	-	-	-	-	-

*The activity at depth Z cm or ρZ g/cm^2 is S(gammas emitted per gram soil per sec) = α/ρ S_A $e^{-(\alpha/\rho)(\rho Z)}$ where S_A = 1.0 gamma/cm^2-s is the total number of gammas emitted in a column of area 1 cm^2 and infinite depth (see equation 3). For α/ρ = 0, S_o/ρ = 1.0 gammas emitted per gram of soil for all Z.

TABLE 8

TOTAL EXPOSURE RATE AT ONE METER ABOVE GROUND FOR NATURAL EMITTERS UNIFORMLY DISTRIBUTED IN THE SOIL

Isotope	μR/h pCi/g	μR/h unit concentration
^{40}K	0.179	1.49 per % K
^{226}Ra+daughters	1.80	0.61 per 0.358×10^{-6} ppm Ra
^{214}Pb	0.20	0.07 " " "
^{214}Bi	1.60	0.54 " " "
^{238}U+daughters	1.82	0.62 per ppm ^{238}U
^{232}Th+daughters	2.82	0.31 per ppm ^{232}Th
^{228}Ac	1.18	0.13 " "
^{208}Tl	1.36	0.15 " "
^{212}Bi	0.09	0.01 " "
^{212}Pb	0.09	0.01 " "
Other	0.09	0.01 " "

Note: Values quoted in reference 1 based on old decay scheme data and buildup factor calculations were:

^{238}U - 0.76 (μR/h)/ppm

^{232}Th - 0.36 (μR/h)/ppm

^{40}K - 1.71 (μR/h)/% K

TABLE 9

TOTAL EXPOSURE RATE (μR/h) AT ONE METER ABOVE GROUND FOR SELECTED FALLOUT ISOTOPES IN THE SOIL

Isotope	Source Activity (mCi/km^2)	(α/ρ) - cm^2/g					
		0.0625	0.206	0.312	0.625	6.25	∞ (Plane)
^{144}Ce	1.0	6.25(-5)	1.34(-4)	1.56(-4)	1.96(-4)	2.86(-4)	3.27(-4)
^{144}Ce+^{144}Pr*	2.0	1.85(-4)	3.51(-4)	4.05(-4)	5.03(-4)	7.22(-4)	8.34(-4)
^{141}Ce	1.0	2.60(-4)	5.23(-4)	6.21(-4)	7.68(-4)	1.15(-3)	1.31(-3)
^{131}I	1.0	1.56(-3)	2.92(-3)	3.35(-3)	4.20(-3)	6.91(-3)	7.28(-3)
^{125}Sb	1.0	1.77(-3)	3.33(-3)	3.82(-3)	4.86(-3)	7.14(-3)	8.29(-3)
^{140}Ba	1.0	7.74(-4)	1.45(-3)	1.69(-3)	2.09(-3)	3.16(-3)	3.66(-3)
^{140}La	1.0	8.98(-3)	1.63(-2)	1.88(-2)	2.40(-2)	3.56(-2)	3.96(-2)
^{140}Ba+^{140}La*	2.15	1.11(-2)	2.02(-2)	2.33(-2)	2.97(-2)	4.40(-2)	4.92(-2)
^{103}Ru	1.0	1.97(-3)	3.66(-3)	4.30(-3)	5.37(-3)	7.90(-3)	9.22(-3)
^{106}Ru+^{106}Rh*	2.0	7.74(-4)	1.43(-3)	1.67(-3)	2.11(-3)	3.17(-3)	3.65(-3)
^{137}Cs	1.0	2.31(-3)	4.29(-3)	4.99(-3)	6.17(-3)	9.24(-3)	1.06(-2)
^{95}Zr	1.0	3.02(-3)	5.51(-3)	6.36(-3)	7.81(-3)	1.17(-2)	1.35(-2)
^{95}Nb	1.0	3.15(-3)	5.74(-3)	6.66(-3)	8.14(-3)	1.24(-2)	1.41(-2)
^{95}Zr-^{95}Nb	3.155	9.91(-3)	1.79(-2)	2.07(-2)	2.54(-2)	3.84(-2)	4.39(-2)
^{54}Mn	1.0	3.40(-3)	6.29(-3)	7.22(-3)	8.88(-3)	1.34(-2)	1.54(-2)
^{60}Co	1.0	9.99(-3)	1.80(-2)	2.06(-2)	2.55(-2)	3.78(-2)	4.32(-2)

*Assuming daughter is in equilibrium with parent-exposure rate is for 1 mCi/km^2 of parent activity.

TABLE 10

ERROR IN 1 METER EXPOSURE RATES FOR INFINITE HALF-SPACE GEOMETRY DUE TO NEGLECTING AIR-SOIL DIFFERENCES (BUILD-UP FACTOR APPROACH)

E (keV)	Soil-Air/Soil-Soil
250	0.79
364	0.87
500	0.90
1000	0.94
1500	0.95
2000	0.96
2500	0.95

TABLE 11

φ/I-(ONE METER) FOR FALLOUT EMITTERS IN THE SOIL - $(\gamma's/cm^2-s)/(\mu R/h)$

Isotope	Eγ (keV)	(α/ρ) - cm^2/g 0.0625	0.206	0.312	0.625	6.25	∞ Plane
^{144}Ce	134	1.04	1.19	1.31	1.48	1.97	2.14
^{144}Ce-^{144}Pr	134	0.352	0.453	0.504	0.577	0.780	0.838
^{141}Ce	145	1.17	1.42	1.52	1.74	2.23	2.45
^{131}I	364	0.444	0.541	0.585	0.636	0.702	0.808
^{125}Sb	428	0.149	0.177	0.193	0.203	0.245	0.259
^{140}La	487	0.046	0.056	0.061	0.064	0.076	0.083
^{140}Ba-^{140}La	487	0.037	0.045	0.049	0.052	0.062	0.067
^{103}Ru	497	0.416	0.503	0.528	0.574	0.687	0.715
^{106}Ru-^{106}Rh	512	0.251	0.303	0.319	0.339	0.401	0.419
^{140}Ba	537	0.296	0.352	0.370	0.400	0.465	0.486
^{140}Ba-^{140}La	537	0.0206	0.0253	0.0268	0.0282	0.0334	0.0362
^{125}Sb	601	0.104	0.121	0.128	0.135	0.160	0.166
^{103}Ru	610	0.0271	0.0322	0.0335	0.0359	0.0430	0.0440
^{106}Ru	622	0.129	0.153	0.160	0.170	0.198	0.207
^{137}Cs	662	0.377	0.440	0.465	0.499	0.582	0.606
^{95}Zr	724	0.155	0.181	0.192	0.206	0.241	0.247
^{95}Zr-^{95}Nb	724	0.0476	0.0557	0.0589	0.0634	0.0734	0.0758
^{95}Zr	757	0.196	0.230	0.242	0.265	0.303	0.313
^{95}Zr-^{95}Nb	757	0.0602	0.0709	0.0744	0.0815	0.0922	0.0961
^{95}Nb	766	0.346	0.409	0.428	0.473	0.531	0.551
^{95}Zr-^{95}Nb	766	0.239	0.282	0.297	0.328	0.371	0.381
^{140}La	816	0.0287	0.0336	0.355	0.0374	0.0433	0.0457
^{140}Ba-^{140}La	816	0.0232	0.0270	0.0286	0.0302	0.0350	0.0368
^{54}Mn	835	0.332	0.380	0.400	0.438	0.497	0.509
^{140}La	1597	0.154	0.166	0.173	0.175	0.195	0.203
^{140}Ba-^{140}La	1597	0.124	0.134	0.140	0.142	0.158	0.163
^{60}Co	1173	0.127	0.146	0.153	0.162	0.183	0.188
^{60}Co	1333	0.134	0.151	0.159	0.168	0.187	0.191

TABLE 12

φ/I – RATIO OF GAMMA-RAY FLUX DENSITY TO EXPOSURE RATE FROM NATURAL EMITTERS IN THE SOIL

Parent Isotope	E_γ (keV)	φ/I $\left(\frac{\gamma's/cm^2\text{-}s}{\mu R/h}\right)$	
Uranium Series, I = 1.82 $\frac{\mu R/h}{pCi/g}$			
^{226}Ra	186	2.52(-3)	
^{214}Pb	242	5.71(-3)	
	295	1.60(-2)	
	352	3.30(-2)	
^{214}Bi	609	5.18(-2)	.0537
	666	1.86(-3)	
	768	6.43(-3)	
	934	4.45(-3)	
	1120	2.31(-2)	
	1238	9.45(-3)	
	1378	8.19(-3)	
	1401-08	6.87(-3)	
	1510	3.91(-3)	
	1730	5.60(-3)	.0395
	1765	2.96(-2)	
	1845	4.35(-3)	
	2205	1.07(-2)	
	2448	3.66(-3)	
Potassium, I = 0.179 $\frac{\mu R/h}{pCi/g}$			
^{40}K	1464	0.203	

Parent Isotope	E_γ (keV)	φ/I $\left(\frac{\gamma's/cm^2\text{-}s}{\mu R/h}\right)$
Thorium Series, I = 2.82 $\frac{\mu R/h}{pCi/g}$		
^{228}Ac	129	1.03(-3)
	210	2.06(-3)
^{212}Pb	239	2.57(-2)
^{234}Ru	241	
^{228}Ac	270	
^{208}Tl	277	3.62(-3)
^{228}Ac	282	
^{212}Pb	301	1.96(-3)
^{228}Ac	338	7.73(-3)
Mixed	328-340	1.03(-2)
^{228}Ac	463	3.26(-3)
^{208}Tl	510	6.84(-3)
^{228}Tl	583	2.27(-2)
^{212}Bi, ^{228}Ac	727	6.60(-3)
^{228}Ac	755	9.57(-4)
	772	1.45(-3)
	795	4.25(-3)
	830+835+840	3.33(-3)
^{208}Tl	860	4.18(-3)
^{228}Ac	911	2.68(-2)
	965+969	2.17(-2)
	1588	4.36(-3)
^{208}Tl	2615	5.92(-2)

TABLE 13

PHYSICAL CHARACTERISTICS OF HASL γ-RAY DETECTORS

Detector No.	514	484	730	785
Type	Closed Coaxial Cylindrical Ge(Li)	Closed Coaxial Cylindrical Ge(Li)	Harshaw Integral Line NaI(Tl)	Harshaw Integral Line NaI(Tl)
Size	4.3 cm×4.4 cm(L)	-	~4"×4"	~4"×4"
Efficiency*	2.17	0.82	37	36
Resolution†	2.3 keV	2.3 keV	52 keV	54 keV
Peak/Compton Ratio‡	30/1	24/1	-	-
Active Volume	~60 cm^3	~25 cm^3	~820 cm^3	~820 cm^3
Drift Depth	~1.7 cm	-	-	-
Bias Voltage	2200 V	2200 V	900 V	900 V

*Counts per unit incident flux at 662 keV.

†FWHM at 662 keV.

‡Evaluated at 1.33 MeV.

TABLE 14

N_o/φ - TOTAL ABSORPTION PEAK COUNTS -
4" × 4" NaI(Tl) DETECTOR[A]

Calibration Source	Energy (keV)	N_o/φ $\frac{cpm}{\gamma/cm^2-s}$ Detector #ED-730	Detector #EA-785	Old 4"×4" Detectors
^{85}Sr	514	2690	2525	3250
^{137}Cs	662	2333	2238	2238
^{54}Mn	835	2075	2060	2400
^{24}Na	1370	1635[B]	168[B]	1900
^{226}Ra	1765	980[C]	970[C]	1150
^{208}Tl	2615	892	970	1140[D]

[A] With $\frac{1}{4}$" bakelite shield.

[B] Inferred from ratio of previous readings to HASL-170 data.

[C] Based on branching ratios in Table 4.

[D] Inferred from 2.73 MeV ^{24}Na line.

TABLE 15

N_o/φ - TOTAL ABSORPTION PEAK COUNTS PER UNIT INCIDENT FLUX - Ge(Li) DETECTORS

Calibration Source	E (keV)	γ's/dis.	Standardized By	N_o/φ $\frac{cpm}{\gamma/cm^2-s}$ 25 cc Ge(Li)	60 cc[a] Ge(Li)
^{241}Am	59.5	0.353	IAEA	276±5	287±7
^{170}Tm	84	0.033	HASL	-	438±25
^{144}Ce	133.5	0.108	HASL	-	596±12
^{141}Ce	145.5	0.490	HASL	-	585±10
^{139}Ce	165	0.80	HASL	-	594±15
^{57}Co	122.1	0.856	IAEA	423±8	565±12
^{198}Au	411.8	0.955	HASL	89.0±4.0	224±3
^{22}Na	511.0	1.81	IAEA	-	171±4
"	1274.5	1.00	IAEA	20.6±1.0	67.0±2.0
^{85}Sr	514.0	0.993	HASL	66.0±3.0	171±4
^{137}Cs	661.6	0.846	HASL-IAEA	49.0±2.0	130±3
^{54}Mn	834.8	1.00	"	33.0±1.0	100±2
^{88}Y	898.0	0.934	HASL	30.0±1.0	97.0±3.0
"	1836.1	0.994	"	13.2±0.5	47.5±1.0
^{65}Zn	1115.5	0.506	"	-	82.0±2.0
^{60}Co	1173.2	0.999	HASL-IAEA	-	74.4±1.0
"	1332.5	1.00	"	-	65.6±1.0
^{24}Na	1368.5	1.0	-	-	63.8[β]
"	2754.1	0.999	-	-	30.4±0.6
^{228}Th	2615	0.36	NBS	-	33.1±1.0

[a] These data fit the following function from 200 keV to 3 MeV with a maximum deviation of ~3%: $\ln N_o/\varphi = 4.48 - 1.03 \ln E$, where E is in MeV.

[β] Normalized

TABLE 16

ANGULAR CORRECTION FACTORS (N_f/N_o)

E (keV)	(α/ρ) - cm²/g: 0	0.206	0.625	∞ Plane
		N_f/N_o - 60 cm³ Ge(Li)		
60	0.69	0.68	0.66	0.65
122	0.94	0.93	0.92	0.90
145	1.00	1.00	0.99	0.97
>155	1.0	1.0	1.0	1.0
		N_f/N_o - 25 cm³ Ge(Li)		
134	0.70	-	-	-
352	0.79	-	-	-
609	0.84	-	-	-
1120	0.91	-	-	-
1765	0.98	-	-	-
		N_f/N_o - 4" × 4" NaI(Tl)		
511	1.14	1.14	1.14	1.14
583	1.12	1.12	1.12	1.12
662	1.11	1.11	1.11	1.11
750	1.10	1.10	1.10	1.10
1464	1.07	-	-	-
1765	1.04	-	-	-
2615	1.02	-	-	-

Total "Energy" - 4" × 4" NaI, N_f/N_o = 1.11

TABLE 17

PEAK AREA PER UNIT EXPOSURE RATE (N_f/I) AND PEAK AREA PER UNIT ACTIVITY (N_f/A) FOR 4"×4" NaI(Tl) DETECTORS[a]

Isotope	E (keV)	α/ρ	No. 730		No. 785		Old Detectors Ref. 5	
			N_f/I[b]	N_f/A[c]	N_f/I[b]	N_f/A[c]	N_f/I[b]	N_f/A[c]
^{238}U	609+665	0	151	275	142	259	150	335
	1765	0	36	66	35	64	45	100
^{232}Th	583	0	64	180	61	171	65	213
	2615	0	59	166	58	165	58	190
^{40}K	1464	0	352	63	344	62	390	80
^{137}Cs	662	0.0625	967	2.24	928	2.15	-	-
		0.206	1129	4.85	1083	4.65	1375	-
		0.312	1193	5.95	1145	5.71	-	-
		0.625	1281	7.90	1228	7.58	-	-
		6.25	1494	13.8	1433	13.2	-	-
		∞	1555	16.5	1492	15.8	-	-
^{95}Zr-Nb[d]	<750>	0.0625	820	7.81	793	7.53	-	-
		0.206	964	17.33	930	16.72	1150	-
		0.312	1018	21.03	980	20.28	-	-
		0.625	1115	28.30	1078	27.30	-	-
		6.25	1266	48.58	1221	46.87	-	-
		∞	1406	57.40	1258	55.37	-	-

[a] With $\frac{1}{4}$" bakelite shield.

[b] cpm/(μR/h)

[c] cpm per pCi/g of in situ soil material including moisture (α/ρ=0) or per mCi/km^2 (α/ρ≠0).

[d] Equilibrium assumed.

TABLE 18

PEAK AREA PER UNIT EXPOSURE RATE (N_f/I) AND PEAK AREA PER UNIT ACTIVITY (N_f/A) FOR Ge(Li) DETECTORS - NATURAL EMITTERS

		60 cc Ge(Li)				25 cc Ge(Li)	60 cc Ge(Li)
Isotope	E(keV)	N_o/φ	N_f/N_o	φ/I	N_f/I*	N_f/A**	N_f/A**
^{40}K	1464	59.8	1.0	0.203	12.1	3.37	2.17
^{238}U	186	510	1.0	2.52(-3)	1.29	0.44	2.35
Series	242	388		5.71(-3)	2.22	0.73	4.04
	295	315		1.60(-2)	5.04	1.58	9.17
	352	255		3.30(-2)	8.42	2.78	15.3
	609	143		5.18(-2)	7.41	2.25	13.5
	666	132		1.86(-3)	0.25	-	0.45
	768	114		6.43(-3)	0.73	0.21	1.33
	934	94.2		4.45(-3)	0.42	-	0.76
	1120	78.0		2.31(-2)	1.80	0.49	3.28
	1238	70.0		9.45(-3)	0.66	-	1.20
	1378	63.3		8.19(-3)	0.52	-	0.94
	1730	50.0		5.60(-3)	0.28	-	0.51
	1765	49.0		2.96(-2)	1.45	0.40	2.64
	2204	39.5		1.07(-2)	0.42	-	0.77
^{232}Th	129	580	1.0	1.03(-3)	0.60	-	1.68
	210	442		2.06(-3)	0.91	-	2.57
	239-41	388		2.57(-2)	9.97	3.28	18.1
	270-82	335		3.62(-3)	1.21	-	3.42
	301	305		1.96(-3)	0.60	-	1.69
	338	260		7.73(-3)	2.01	0.68	5.67
	328-40	265		1.03(-2)	2.73	-	7.70
	463	195		3.26(-3)	0.64	-	1.79
	510	176		6.84(-3)	1.20	-	3.39
	583	154		2.27(-2)	3.50	1.1	9.86
	727	122		6.60(-3)	0.81	-	2.27
	755	118		9.57(-4)	0.11	-	0.32
	772	115		1.45(-3)	0.17	-	0.47
	795	112		4.25(-3)	0.48	-	1.34
	830-40	108		3.33(-3)	0.36	-	1.01
	860	103		4.18(-3)	0.43	-	1.21
	911	97.0		2.68(-2)	2.60	0.71	7.33
	965+69	91.0		2.17(-2)	1.97	0.53	5.57
	1588	54.7		4.36(-3)	0.24	0.063	0.67
	2615	32.8		5.92(-2)	1.94	-	5.48

*cpm/(μR/h)

**cpm/(pCi/g)

TABLE 19

PEAK AREA PER UNIT EXPOSURE RATE (N_f/I)* FOR 60 cc Ge(Li) DETECTOR-FALLOUT

Isotope	E(keV)	N_o/φ	(α/ρ) - cm^2/g 0.0625	0.206	0.312	0.625	6.25	∞ Plane
^{144}Ce-Pr**	134	596	208	267	294	337	451	479
^{141}Ce	145	585	678	831	880	998	1278	1390
^{131}I	364	250	111	135	146	159	201	202
^{126}Sb	428	210	31.3	37.2	40.5	42.6	51.5	54.4
	601	145	15.1	17.5	18.6	19.6	23.2	24.1
^{140}Ba	537	162	48.0	57.0	59.9	64.8	75.3	78.7
^{140}La	487	180	8.28	10.1	11.0	11.5	13.7	14.9
	1597	55	8.47	9.13	9.52	9.63	10.7	11.2
^{103}Ru	497	180	74.9	90.5	95.0	103	124	129
^{106}Ru-^{106}Rh	512	175	32.3	53.0	55.8	59.3	70.2	73.3
	622	140	18.1	21.4	22.4	23.8	27.7	29.0
^{137}Cs	662	130	49.0	57.2	60.5	64.9	75.7	78.8
^{95}Zr	724	122	18.9	22.1	23.4	25.1	29.4	30.1
	757	117	22.9	26.9	28.3	31.0	35.5	36.6
^{95}Nb	766	114	39.4	46.6	48.8	53.9	60.5	62.8
^{54}Mn	835	106	20.1	40.3	42.4	46.4	52.7	54.0

*cpm/(μR/h); for N_f/A multiply values by I from Table 9.

**Equilibrium assumed.

Table 20

"ENERGY" BAND EQUATIONS FOR NaI(Tl) DETECTORS

"Energy" Bands

ΔE_1	1.32 MeV to 1.60 MeV
ΔE_2	1.62 MeV to 1.90 MeV
ΔE_3	2.48 MeV to 2.75 MeV
ΔE_{Total}	0.15 MeV to 3.4 MeV

Exposure Rate Equations

Detector #730	Detector #785
$K = .085\ E_1' - .060\ E_2' - .024\ E_3'$	$K = .087\ E_1' - .061\ E_2' - .024\ E_3'$
$U = .421\ E_2' - .224\ E_3'$	$U = .433\ E_2' - .230\ E_3'$
$T = .292\ E_3'$	$T = .297\ E_3'$
$I = E_T'/37.9$	$I = E_T'/36.5$

where K, U, T, are the exposure rates in μR/h for ^{40}K, the ^{238}U series, the ^{232}Th series, respectively, and I is the total exposure rate. E_1', E_2', E_3', E_T are respectively the total "energy" in BeV/20 min. in ΔE_1, ΔE_2, ΔE_3, ΔE_{Total} (see text) corrected for cosmic ray exposure.

Cosmic Ray Response - BeV/20 min.

Altitude	E_1	E_2	E_3	E_{Total}
0'	0.40	0.35	0.30	7.7
1000'	0.42	0.37	0.32	8.2
2000'	0.46	0.40	0.34	8.9
3000'	0.52	0.45	0.36	9.8
4000'	0.60	0.53	0.38	11.0
5000'	0.70	0.63	0.41	12.8
8000'	1.28	1.10	0.94	24.7

TABLE 21

EXAMPLES OF FIELD SPECTROMETRIC MEASUREMENTS MADE WITH Ge(Li) DETECTORS AND NaI(Tl) DETECTORS

Location	Detector Type	μR/h							
		K	U	T	Cs	Zr-Nb	Other	Sum	Ion Chamber
Joliet, Ill. 1971	Ge(Li)	2.8	1.2	2.5	0.2	0.3	0.1	7.1	7.8
	NaI(Tl)	2.7	1.1	2.4	0.3	0.2	-	6.7	
Channahan, Ill. 1971	Ge(Li)	2.6	1.0	1.9	0.2	0.3	0.1	6.1	5.9
	NaI(Tl)	2.4	1.1	1.8	0.2	0.2	-	5.7	
Morris, Ill. 1971	Ge(Li)	2.2	1.4	1.7	0.1	0.3	<0.1	5.7	-
	NaI(Tl)	2.2	1.2	1.8	0.1	0.2	-	5.5	
Waterford, Conn. 1971	Ge(Li)	1.7	1.7	3.0	0.6	0.2	-	7.2	7.6
	NaI(Tl)	1.7	1.4	3.4	0.4	0.1	-	7.0	
Waterford, Conn. 1971	Ge(Li)	2.4	1.6	2.9	0.7	0.2	-	7.8	8.0
	NaI(Tl)	2.4	2.1	3.1	0.4	0.1	-	8.1	
Forked River, N. J. 1971	Ge(Li)	0.2	0.8	0.9	0.6	0.2	-	2.7	2.6
	NaI(Tl)	0.2	0.9	0.8	0.7	0.2	-	2.8	
Forked River, N. J. 1971	Ge(Li)	0.3	0.5	0.6	0.8	0.1	-	2.3	2.1
	NaI(Tl)	0.3	0.5	0.5	0.8	0.1	-	2.2	
Denver, Colo. 1965	NaI(Tl)	3.4	2.4	7.4	0.3	-	0.2	13.7	13.8
Bikini, Atoll 1967	NaI(Tl)	0	0	0	19.0	-	5.8	24.8	24.0

TABLE 22

ROUGH COMPARISONS OF FIELD SPECTROMETRIC ESTIMATES OF ^{137}Cs SOIL ACTIVITY WITH NEARBY ^{90}Sr SOIL SAMPLE MEASUREMENTS

Site	Soil Sampling Date	Field Measurement Date	mCi/km² Inferred from Soil Sample	mCi/km² Field Spectrum	Notes
Fort Collins, Colo.	4/65	9/65	80	50	*A,B,C*
Salt Lake City, Utah	9/65	8/65	157	58	*A,B,C*
Derby, Colo.	9/65	8/65	93	77	*A,B,C*
Rapid City, S.D.	9/65	8/65	147	127	*A,B,C*
New Orleans, La.	3/66	9/65	76	62	*A,B,C*
Beltsville, Md.	11/65	11/65	95±15	109	*D*

Notes:

A The ^{137}Cs soil activity was inferred from a radiochemical determination of ^{90}Sr by multiplying by 1.5.

B The field spectral analysis assumed $\alpha/\rho = 0.206$ for all sites, which may be too large since all the field spectrometric values are lower than the values referred from the samples.

C Except for Fort Collins the soil sampling and field spectrometric sites are not identical but are in the nearby vicinity of each other.

D Using measured depth distribution - actual ^{137}Cs soil analysis.

TABLE 23

CONVERSION FACTORS AND OTHER DATA USEFUL FOR FIELD SPECTROMETRY

1 μR/h = 65.9 MeV/g-s
1 mrad/y = 0.130 μR/h
1 μR/h = 7.65 mrad/y
1 mCi/mi^2 = 0.386 mCi/km^2
3.361 × 10^{-7} curies/g ^{238}U
1.09 × 10^{-7} curies/g ^{232}Th
0.988 curies/g ^{226}Ra
3.30 gammas/s(1.46 MeV)-g Potassium
1 dpm = 0.45 pCi

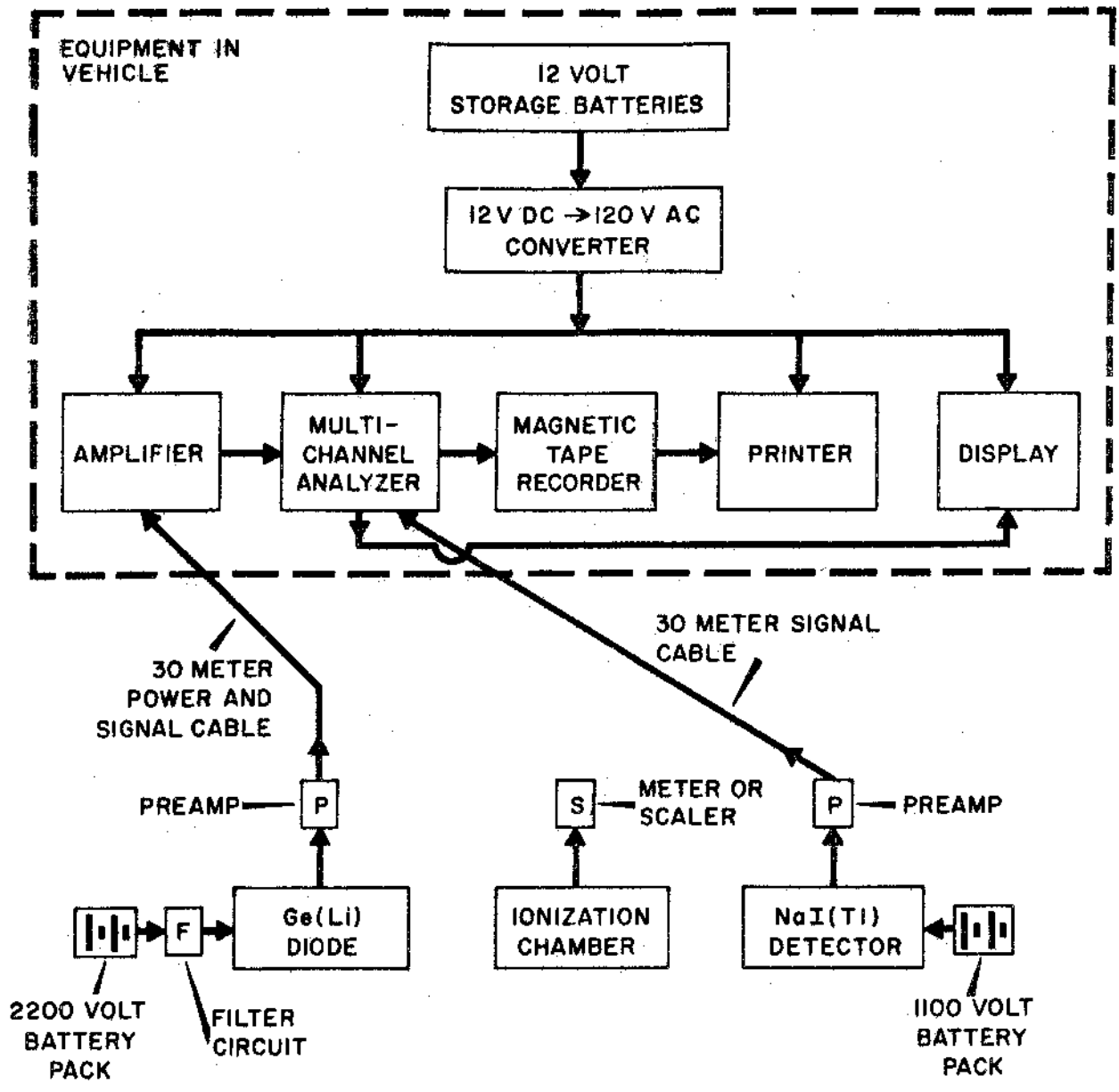

HASL FIELD SPECTROMETRIC SYSTEMS

Figure 1. Diagram of field spectrometers and ionization chamber.

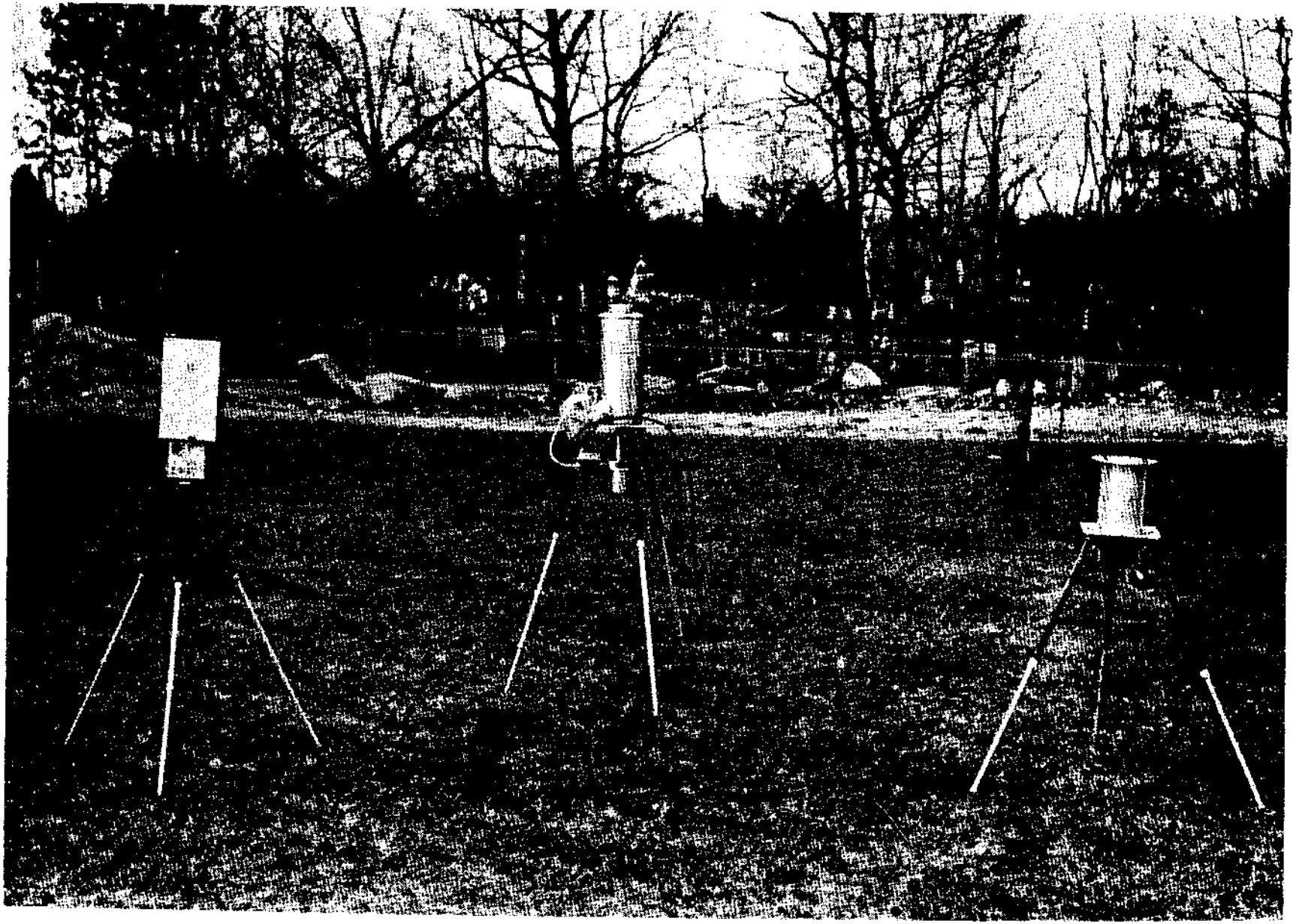

Figure 2. Field equipment showing, left to right, ionization chamber, Ge(Li) detector and NaI(Tl) detector

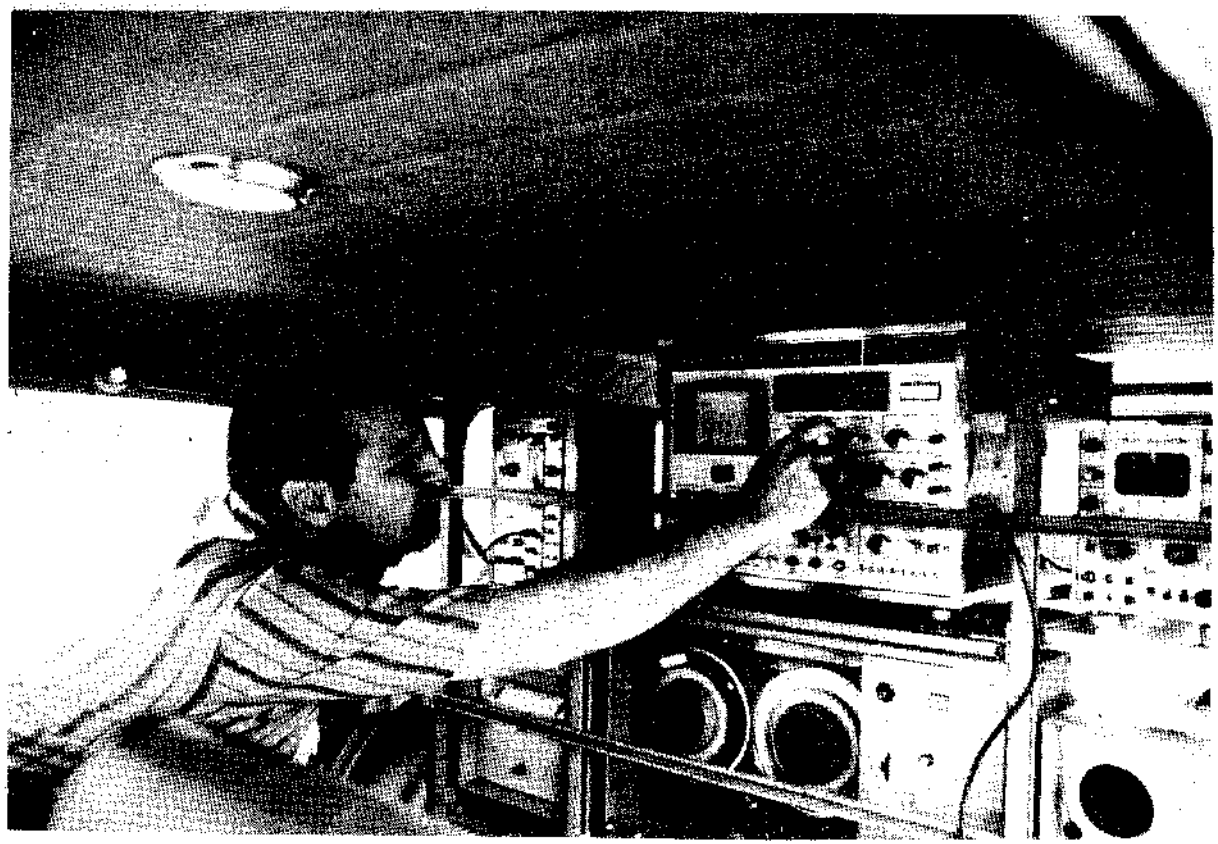

Figure 3. Electronic equipment in rack in standard station wagon.

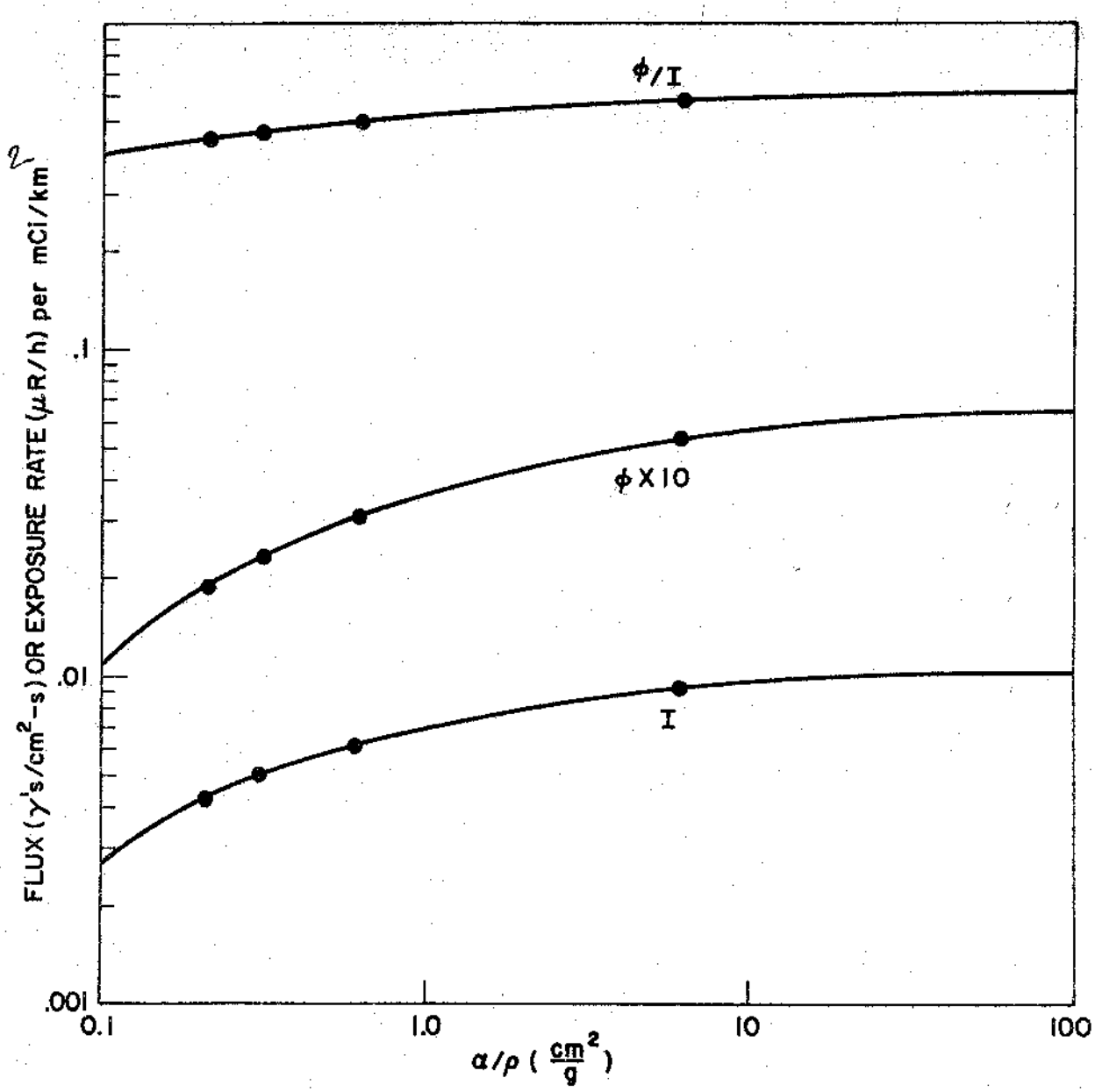

Figure 4. φ, φ/I, and I at one meter above the ground vs α/ρ source depth distribution.

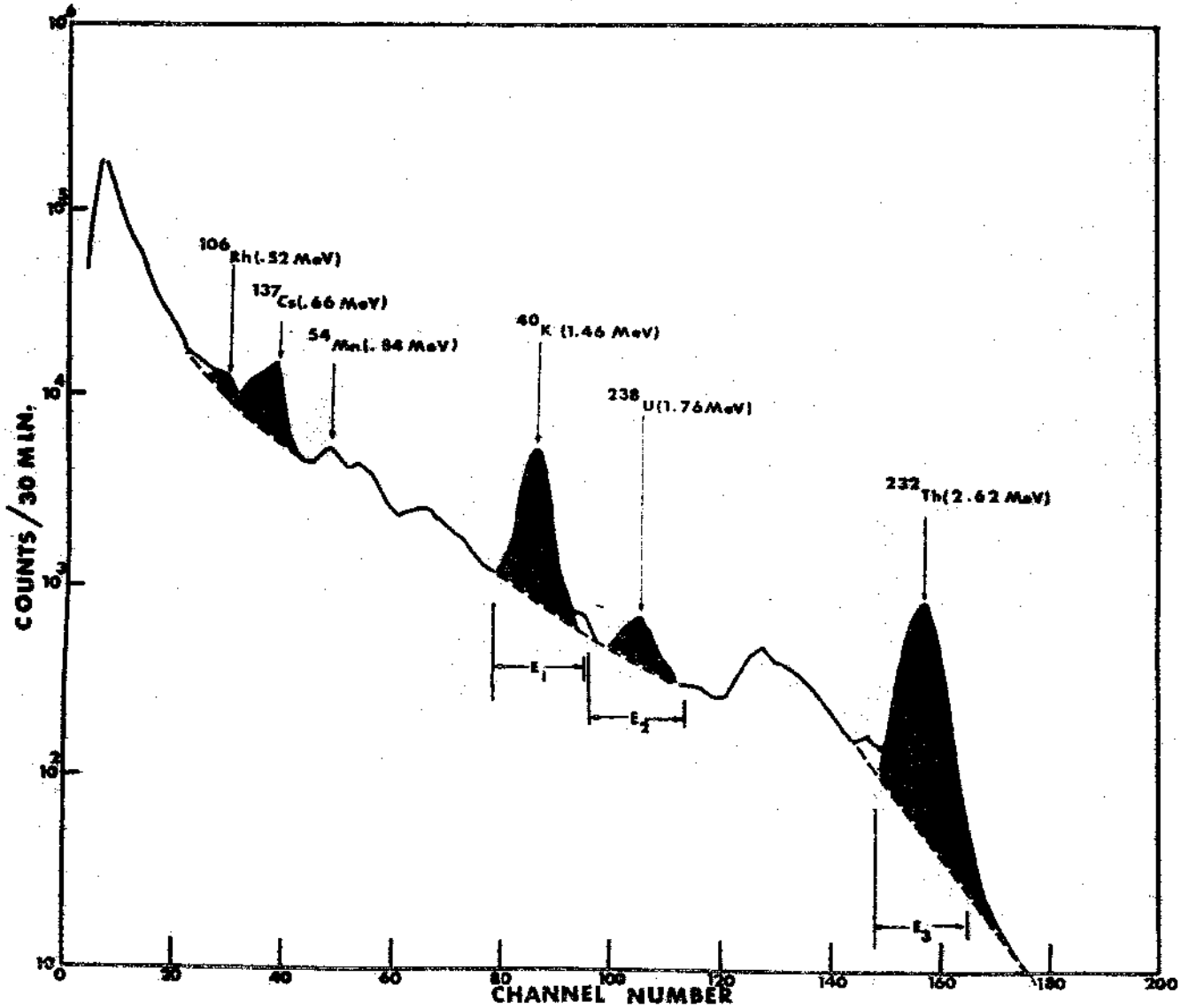

Figure 5, NaI field spectrum. Shaded areas indicate our estimates of the peak area used to determine the total exposure rate due to indicated isotope and and daughters. E_1, E_2 and E_3 are the 3 bands used for determining natural gamma exposure rates.

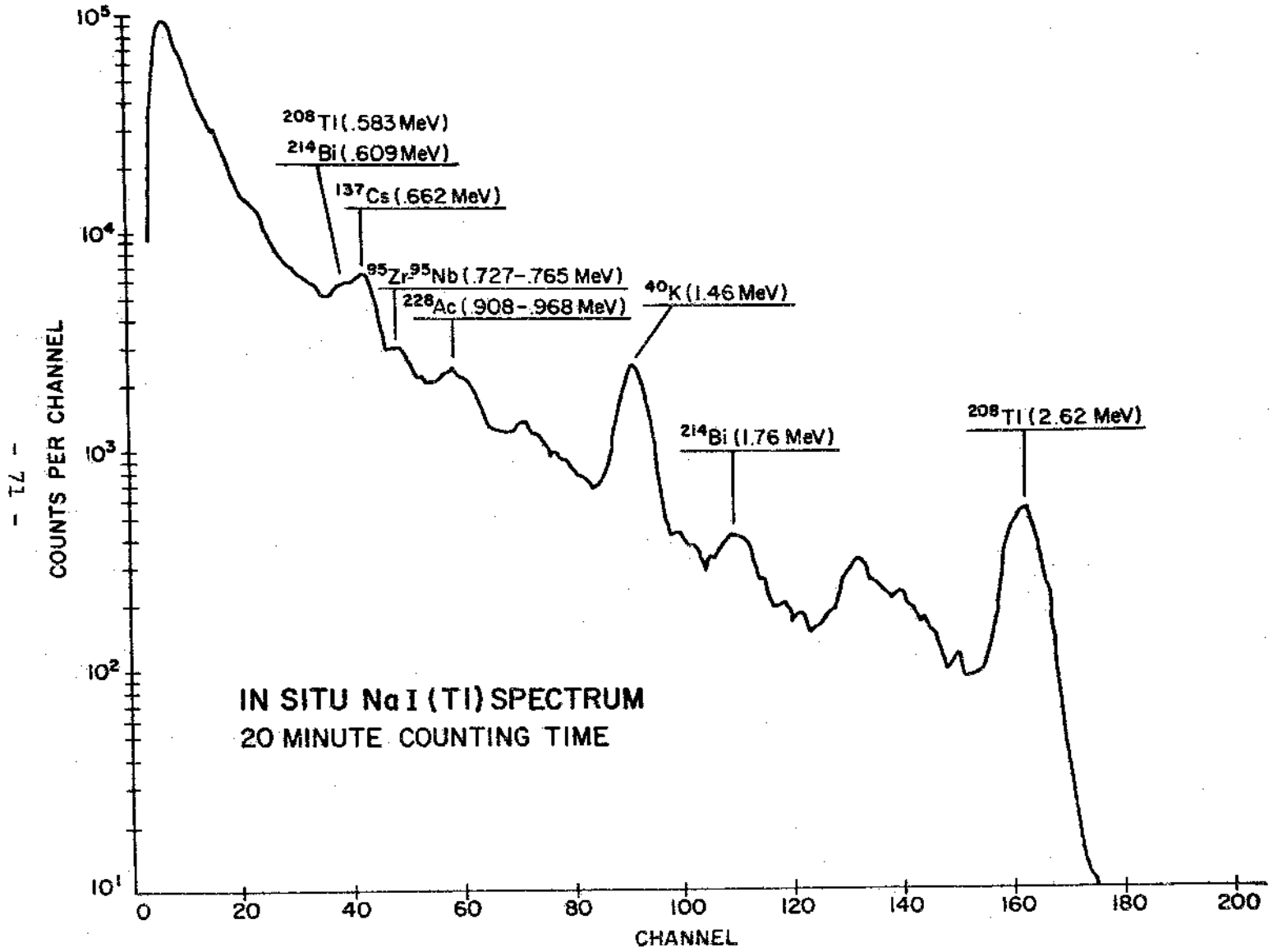

Figure 6. In situ spectrum, northeastern U.S.A. location, taken in 1971 with 10 cm by 10 cm NaI(Tl) crystal, 20 minute counting time.

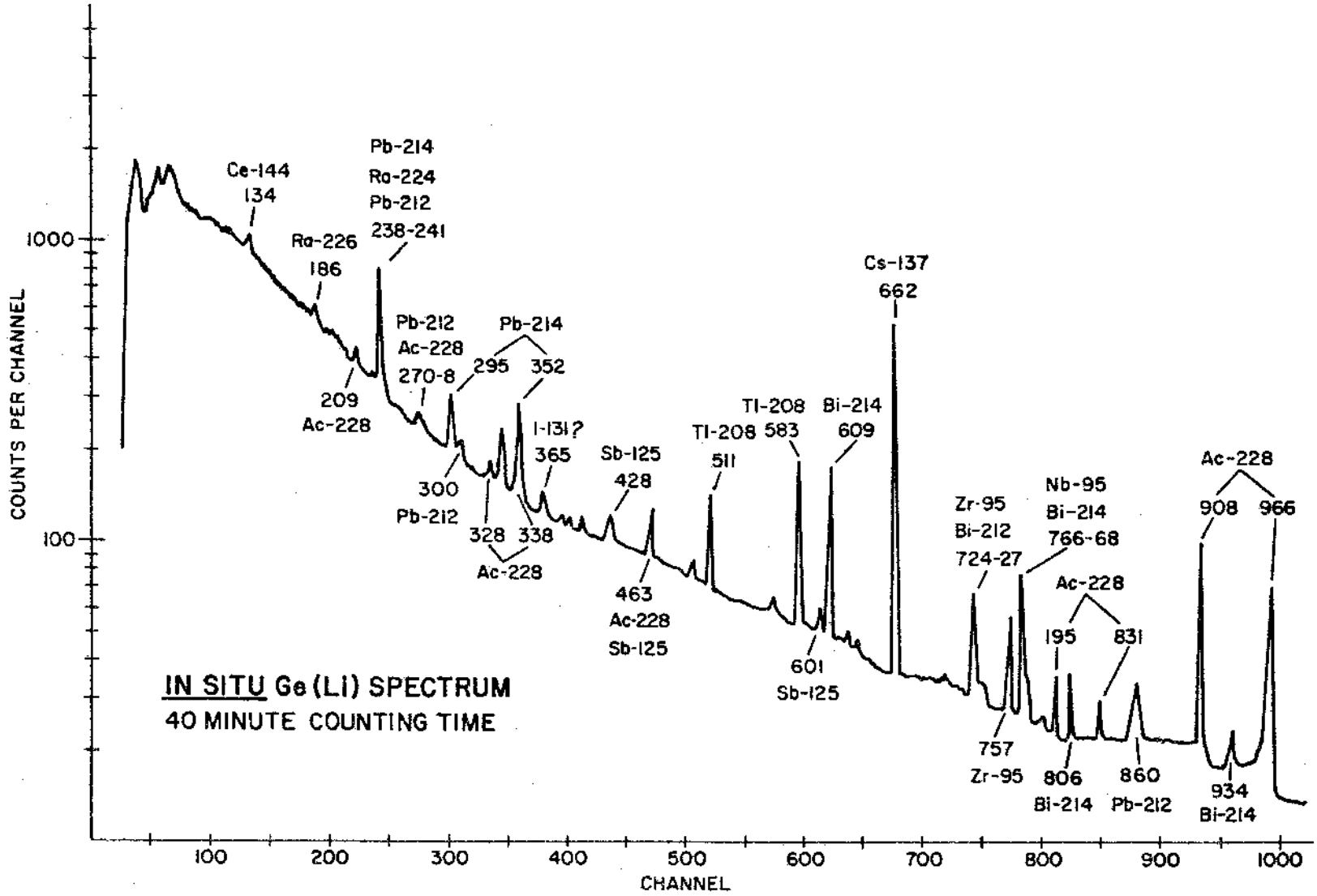

Figure 7. In situ spectrum, taken with that in Figure 6 with 60 cm^3 Ge(Li) detector, 40 minute counting time. Photon energies in keV.

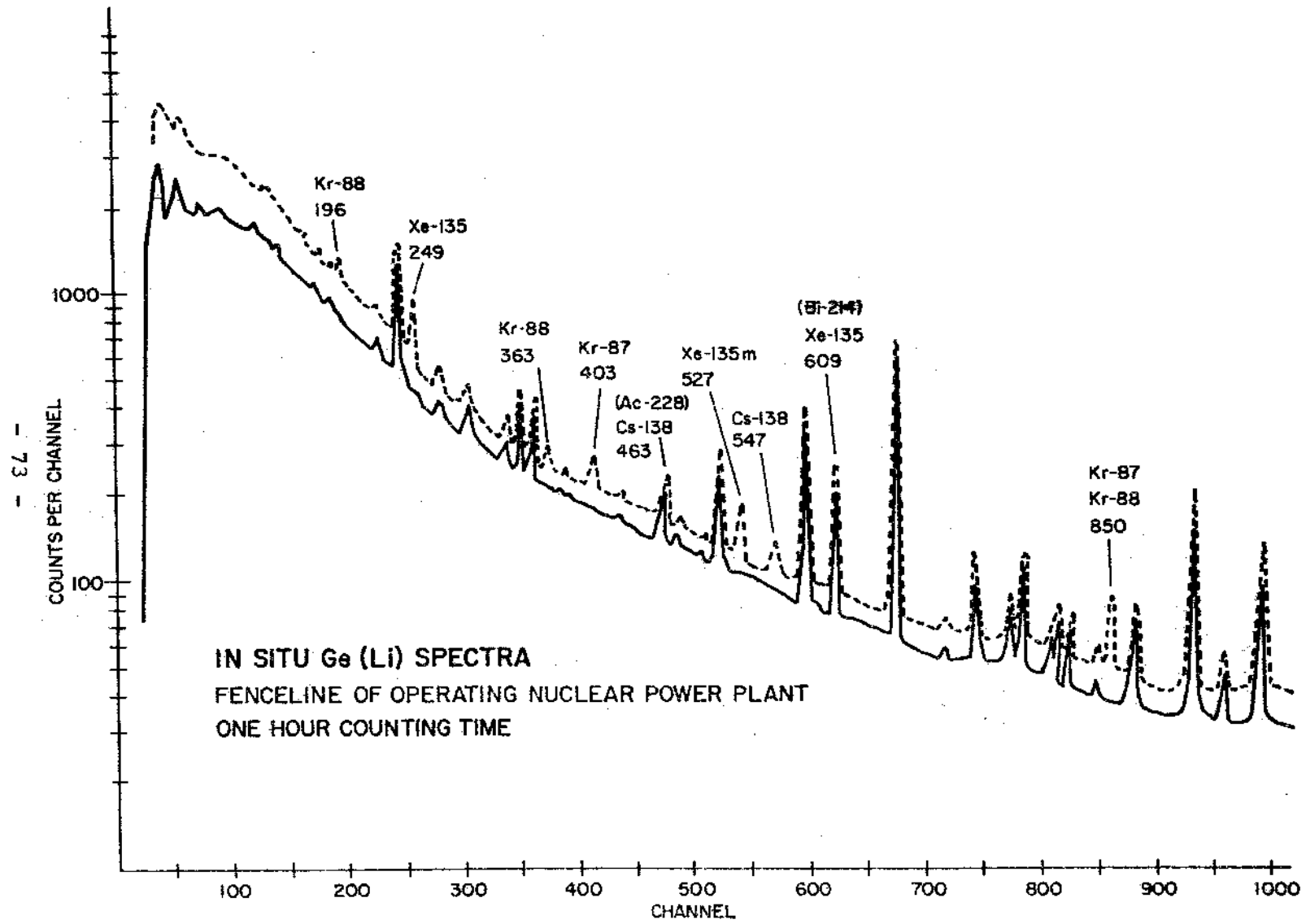

Figure 8. In situ Ge(Li) spectra at fenceline of boiling water reactor. Upper spectrum with gaseous plume overhead; bottom spectrum with wind blowing away from detector.

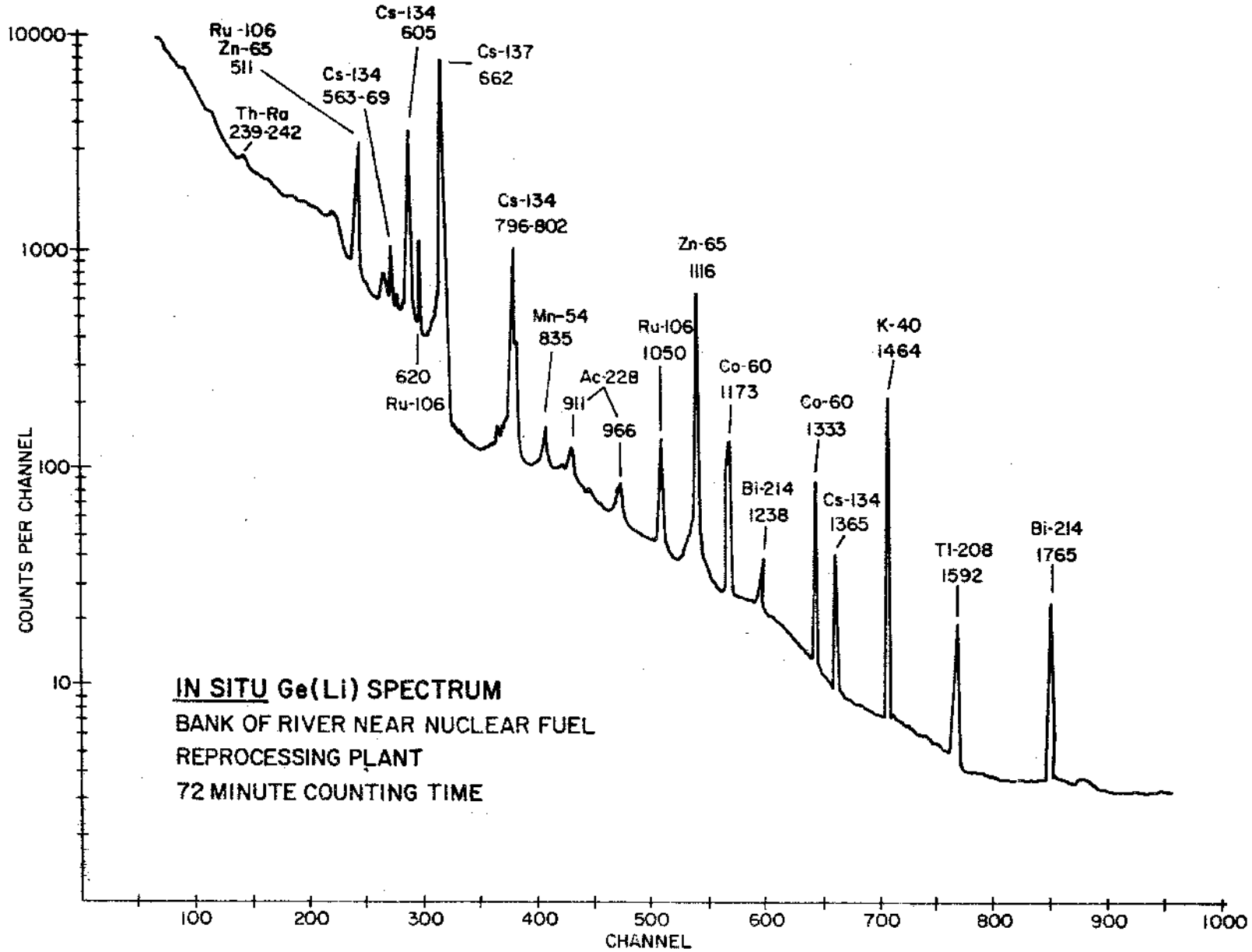

Figure 9. In situ 25 cm^3 Ge(Li) spectrum on river bank near fuel reprocessing plant, 72 minute counting time.

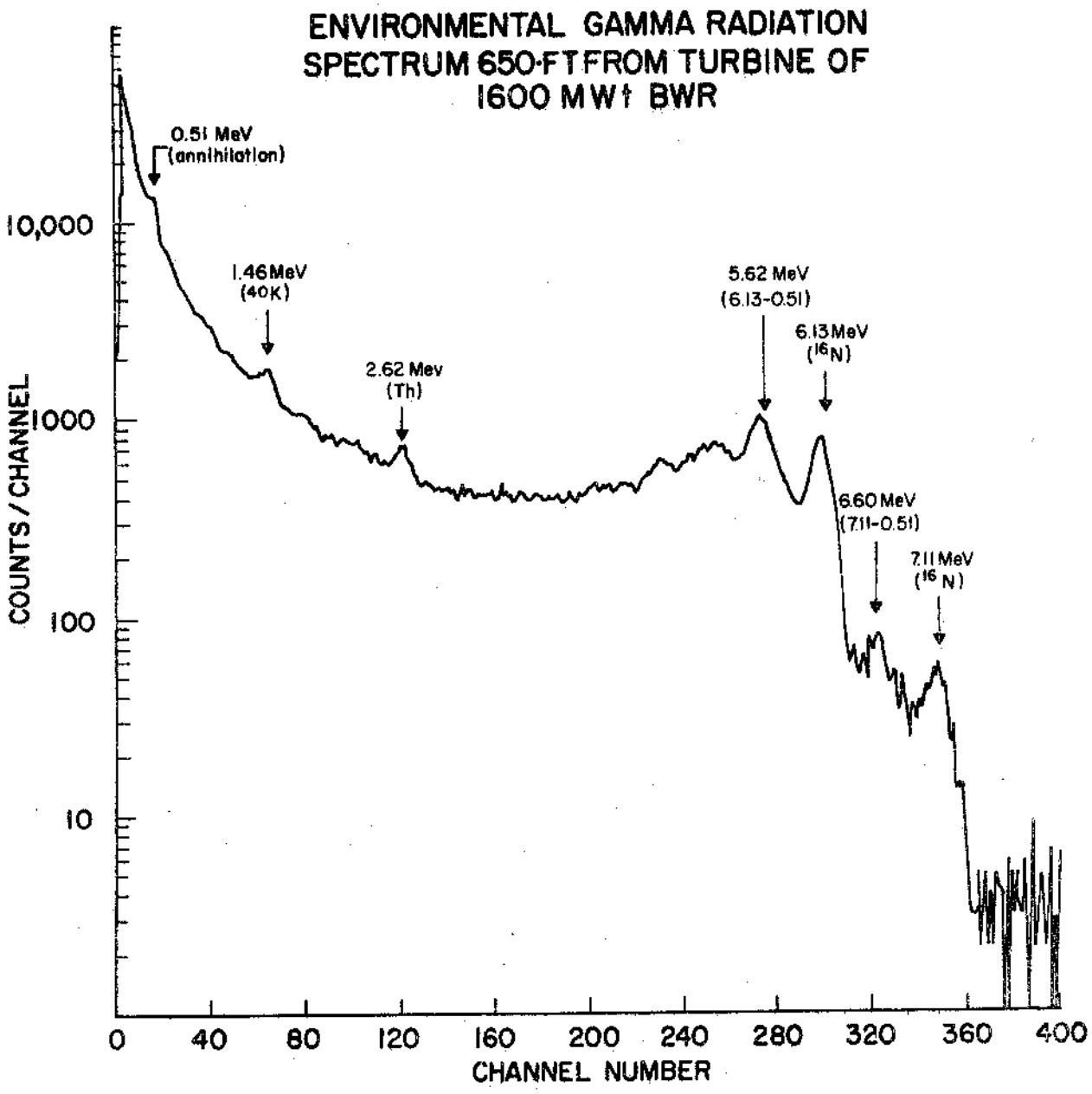

Figure 10. In situ NaI(Tl) spectrum 650 feet from turbine of a 1600 - MWT_{Th} BWR.